Rift and plume: a discussion on active and passive rifting mechanisms in the Afro-Arabian rift based on synthesis of geophysical data

Ran Issachar[1,2], Peter Haas[1,3], Nico Augustin[3] and Jörg Ebbing[1]

[1]Institute for Geosciences, Kiel University, Geophysics, Kiel, Deutschland, [2]Geological Survey of Israel, Jerusalem, Israel, [3]GEOMAR Helmholtz Centre for Ocean Research, Kiel, Deutschland

Correspondence to: Ran Issachar (ranis@gsi.gov.il)

Abstract

The causal relationship between the activity of mantle plumes and continental break-up is still elusive. The Afro-Arabian rift system offers an opportunity to examine these relationships, in which an ongoing continental break-up intersects a large Cenozoic plume-related flood basalt series. In the Afar region, the Gulf of Aden, the Red Sea, and the Main Ethiopian Rift form an R-R-R triple junction, separating the Ethiopian and Yemen Traps by ~600 km. We provide an up-to-date synthesis of the available geophysical and geological data from this region. We map the rift architecture in the intersection region of the rifts and review the spatio-temporal constraints in developing the different features of the plume-rift system.

We infer two spatial constraints in the development of the rifts: (1) the connection of the Main Ethiopian Rift to the Gulf of Aden and the Red Sea by its northeastward propagation; (2) the abandonment of an early tectonic connection between the Red Sea and the Gulf of Aden. Additionally, chronological evidence suggests that regional uplift and flood basalt eruptions sufficiently preceded rifting. By this, we infer a progressive development in which the onset of the triple junction marks a tectonic reorganization and was the last feature to develop after all rift arms were thoroughly developed. We argue that the classical active and passive rifting mechanisms cannot simply explain the progressive development of the Afro-Arabian rift and propose a scenario of plume-induced plate rotation that includes an interaction between active and passive mechanisms. In this scenario, the arrival of the Afar plume provided a push force that promoted the rotation of Arabia around a nearby pole, enabling the rifting and, ultimately, the break-up of Arabia from Africa.

Short summary:

We explore the causal relationship between the arrival of the Afar plume and the initiation of the Afro-Arabian rift. We mapped the rift architecture in the triple junction region from geophysical data and reviewed the available geological temporal evidence. We infer a progressive development of the plume-rift system and suggest an interaction between active and passive mechanisms in which the plume provided a push-force that changed the kinematics of the associated plates.

1. Introduction

The causal dependency between the eruption of flood basalts and continental break-up is still unclear, although a close occurrence between these two phenomena has been recognized for a long time.

Continental flood basalts, often referred to as traps, form large igneous provinces covering huge continental areas (Bryan and Ferrari, 2013; Ernst, 2014). Continental flood basalts are often associated with extensive volcanism during short time intervals, which are brought to the surface by deep-seated mantle plumes (Richards et al., 1989; White and McKenzie, 1995; Koppers et al., 2021), although other mechanisms were also suggested (e.g., Anderson, 1994, 2005).There is evidence for a close temporal and spatial occurrence between the eruption of flood basalts and continental break-up. In particular, when reconstructed back to their original plate tectonic configuration, an R-R-R triple junction is typically found within the flood basalt areas (Morgan, 1971; Burke and Dewey, 1973; Buiter and Torsvik, 2014). Using the geological record to examine the mutual dependency of these processes is challenging. It requires high-precision constraints regarding the temporal and spatial development of the different volcanic and tectonic features, often obscured by the long geological history.

The Afar region in the central parts of the Afro-Arabian rift system is recognized as a key locality to examine models of plume-rift association, offering a young and active case study in which plume, regional uplift, R-R-R triple junction, break-up, and oceanic spreading co-exist and are superimposed (Fig. 1). Plume-rift association is mainly explained by either 'active' (e.g., Sengör and Burke, 1978) or 'passive' (e.g., White and McKenzie, 1989) views, with no interaction between those modes. However, some evidence suggests a more complex effect of plumes on the regional plate kinematics (e.g., Cande and Stegman, 2011). Despite the contrary implications of the 'active' and 'passive' views, the Afar case study was used as a prime example to support both, and some authors argued that both processes are required to explain the observations (Burke and Dewey, 1973; White and McKenzie, 1989; Courtillot et al., 1999). The discrepancy can be primarily attributed to a lack of accurate geological and geophysical evidence, leading to contrary interpretations.

The purpose of this paper is to utilize a synthesis of the available geological and geophysical data from the Afar region and to use it for geodynamic implications in the study area. We first review the evidence regarding the temporal association of the volcanic and rift components of the system. This review is essential because large amounts of new data were collected in recent years, enabling a re-examination of the relationships between the plume and the rifting. We further provide an analysis and interpretation of modern geophysical datasets, including topography, bathymetry, gravity, magnetic anomalies, earthquakes, and volcano distribution. Using these datasets, we map the architecture of the rift margins and axes and infer spatial constraints in developing the rift segments. Finally, we discuss the results in the light of recent models and other case studies in the world, aiming to shed light on the causal relationship between mantle plumes and tectonic processes in the crust.

2. Active and passive mechanisms for plume-rift association

The existence of deep mantle convection and its interaction with the Earth's lithosphere was already pointed out by Wilson (1963), and a close occurrence to continental break-up was soon noticed by the abundance of hotspots near many rift junctions (Morgan, 1971) and flood basalt volcanism along passive margins (Richards et al., 1989). Although Morgan (1971) speculated that deep mantle convection has a significant role in accelerating the overlying tectonic plates, it was later realized that slab-pull provides the main driving force for plate motion (Forsyth and Uyeda, 1975). In their landmark paper, Burke and Dewey (1973) presented 45 case studies of rift junctions associated with hot spots. They proposed a model in which plume-associated uplift and volcanism precede and generate the rift arms, initiated from a triple

junction within the plume region. Afar was used as a first and prime example, highlighting its importance as a young and active case study; however, they already noted its complexity (Burke and Dewey, 1973).

Following these insights, 'active' rifting models were developed to explain plume-rift associations (e.g., Keen, 1985; Moretti and Froidevaux, 1986; Campbell and Griffiths, 1990; Hill, 1991; White and McKenzie, 1995). These models generally propose that rifting can result from a combination of processes derived from the actively rising head of an anomalously hot mantle. These include impinging and eroding the base of the lithosphere, which prompts uplift and decompression melting, which in turn introduces internal extensional forces and ultimately leads to break-up. Accordingly, in this view, regional uplift and volcanism are expected to precede rifting, which would initiate from a triple junction above the mantle plume head (Fig. 2a).

Later contributions challenged the active view, arguing that a 'passive' asthenospheric upwelling can also resolve the occurrence of flood basalt near rifts (firstly introduced by White and McKenzie, 1989). In this view, rifting is initiated by the remote stresses, usually along former sutures and weak zones, regardless of underlying plumes. The production of massive volcanism is allowed when the thinned and stretched lithosphere is underlaid by a thermal anomaly in the mantle. The volcanism is generated by decompression melting of the hot asthenospheric mantle, passively rising. As plumes form large areas of higher temperatures in the mantle, massive volcanism is found on Earth's crust close to rifts. Accordingly, in this view, subsidence is a precondition required for magmatism, and there is no particular reason for a triple junction to form within the flood basalts region (Fig. 2b).

Although active and passive views have been discussed in the last 50 years, the role of plumes in initiating rifting is still unclear and much debated. Even for well-studied and prime examples of plume-rift association as the Siberian, Parana-Etendeka, Deccan, and Greenland traps, there is no agreement on whether active processes initiated rifting (Geoffroy, 2005; Ivanov et al., 2015; Frizon De Lamotte et al., 2015; Fromm et al., 2015; Mitra et al., 2017). Some authors emphasize the significance of preexisting lithosphere weaknesses along structural inheritance and former sutures (Buiter and Torsvik, 2014; Will and Frimmel, 2018), while others show the potential of plumes to thermally and chemically erode the base of the lithosphere in the weakening process allowing rifting (Sobolev et al., 2011). Additionally, some models demonstrate that mixed active-passive scenarios can better explain observation (Koptev et al., 2018), and even that both mechanisms are needed to explain temporal variations in rifts (Huismans et al., 2001).

In addition to the dichotomic views, some evidence implies more complex relationships between plumes and the kinematics of the associated plates (van Hinsbergen et al., 2011; Cande and Stegman, 2011; Chatterjee et al., 2013; Pusok and Stegman, 2020). These studies discuss the role of plumes in changing the relative motions of the overlying plates and suggest that lateral forces, induced by the arrival of the plume head, can add up to the remote stresses, change the plate kinematics and even trigger the formation of new plate boundaries (van Hinsbergen et al., 2021) (Fig. 2c). Thus, in this view the plume is changing the remote stress field, which in-turn allows rifting.

3. Geological setting

The Afro-Arabian rift system extends from Turkey to Mozambique (McConnell and Baker, 1970) and is the current episode of the Phanerozoic break-up of the East African continental plate (Bosworth, 2015). It

contains rifting in the Gulf of Aden, in the Red Sea, and in East Africa. In the center of that system, the Ethiopian northwestern and southeastern plateaus represent an elevated topography with a highest peak of 4,620 m (Ras Dashan) and an average elevation of 2000 m above sea level. This area is part of the so-called African Superswell, a wide region of anomalously high topography comprising East Africa (Lithgow-Bertelloni and Silver, 1998; Corti, 2009). In western Yemen, the Sarawat Mountains are the highest peaks in the Arabian Peninsula, reaching more than 3,000 m, at only 100 km from the shoreline of the Red Sea. The mountains show a typical stair morphology with steep slopes at the western and southern sides, while the eastern side slopes downward more gently.

The Gulf of Aden is the most developed rift segment in the Afro-Arabian rift, with a mature and fully developed oceanic spreading center connected to the mid-ocean ridge in the Indian Ocean. Six pairs of magnetic anomalies associated with seafloor spreading are recognized along the Gulf of Aden (Fournier et al., 2010) (Fig. 3). Oblique rifting and high-angle structural inheritance along the Gulf of Aden resulted in multiple ridge segments and fracture zones (i.e., transform faults; Leroy et al., 2013; Autin et al., 2013; Bellahsen et al., 2013; Duclaux et al., 2020).

At the northern parts, rifting in the Red Sea is connected by the Dead Sea Fault to the Eurasian collision zone along the Taurus-Zagros Mountains. The Red Sea is experiencing the last stages of break-up and early stages of oceanic accretion. An oceanic spreading center with three pairs of ridge parallel magnetic anomalies is developed in the southern parts of the Red Sea (Schettino et al., 2016) (Fig. 3). However, oceanic crust is probably flooring most of the basin (Augustin et al., 2021).

The Main Ethiopian Rift is the northernmost section of the intra-continental rifting in East Africa, splitting the not-yet well-individualized Somali plate from Africa (Chorowicz, 2005). Current rifting in the Main Ethiopian Rift is characterized by a narrow rift valley, in which volcanic and tectonic activities are localized and influenced by oblique rifting conditions (Corti, 2009).

The Afar triangle is where the above-mentioned three rift arms meet (Fig. 3). It is considered a geological depression as it is an area of low elevation compared to the high Ethiopian plateaus, and thus commonly referred to as the Afar 'depression'. Nevertheless, this term is misleading as the Afar triangle is included within the rifted area and is geologically elevated from the deep bathymetry of the Gulf of Aden and the Red Sea basins. The Afar triangle is mainly floored by Pliocene and younger volcanic rocks, where Miocene volcanic series are exposed along the western margins and at the elevated Danakil block. It comprises many volcanoes that compose axial volcanic ranges (Fig. 2), where the Red Sea side is characterized by transverse volcanic fields and the southern side by central volcanoes (Varet, 2018). Two symmetric magnetic anomalies have been recognized in the Tendaho graben, similar to those observed along spreading centers in the Gulf of Aden (Bridges et al., 2012). These could be associated either with young oceanization or with linear anomalies developed in transitional crust (Ebinger et al., 2017). Structurally, several mega-scale accommodation zones connecting the different rift segments and a triple junction location are recognized at 11.0°N, 41.6°E at the Tendaho-Goba'ad Discontinuity (e.g, Tesfaye et al., 2003) (Fig. 3).

4. Temporal constraints

4.1. Flood basalts and uplift

Vast efforts were made to study the chemistry and chronology of flood basalts in East Africa (see review by Rooney, 2017). Two phases of extensive flood basalt volcanism are associated with plume-lithosphere interaction (Fig. 4). The early phase is mainly confined to southern Ethiopia and northern Kenya. The timing of this event is poorly constrained to 45-35 Ma (George et al., 1998). The second phase of flood basalt eruptions was more voluminous, more widespread, and shorter-lived. Earliest basalts of this phase date back to 34 Ma near Tana Basin, Ethiopia (Prave et al., 2016) and 31 Ma in western Yemen (Peate et al., 2005) (Fig. 4). The traps accumulated very rapidly, in less than 6 Ma (Coulié et al., 2003), and include tholeiitic to alkaline compositions of asthenosphere mantle source (Mattash et al., 2013). Thick sequences of up to 2 km are observed within a widespread region in Ethiopia and Kenya (Bellieni et al., 1981; Wescott et al., 1999; McDougall and Brown, 2009). It is commonly accepted that these flood basalts are of a deep-seated mantle plume origin (Koppers et al., 2021). However, the mechanism is debatable and may involve multiple plume impingements within a broad upwelling zone connected to the African superplume in the lower mantle (Meshesha and Shinjo, 2008) or a single plume-lithosphere interaction (Rooney, 2017).

An elevated topography is associated with the eruption of the flood basalts in Ethiopia. The flood basalts are almost exclusively positioned within the elevated regions of the Ethiopian and Somalian plateaus and the Sarawat Mountains in southwest Yemen (Fig. 1). Dynamic topography component supports up to 1 km of present-day elevation of the Ethiopian and Somalian plateaus, confirming the significant contribution of mantle convection to the regional uplift (Gvirtzman et al., 2016). Although the uplift chronology is not easily resolved, recent studies infer it is a long-term feature already present before the emplacement of the flood basalts (Sembroni et al., 2016; Faccenna et al., 2019). Regional uplift is estimated to begin before 40 Ma, with maximal uplifts between 12 and 28 Ma, reaching an average elevation of 2500 m (Fig. 4) (Sembroni et al., 2016).

4.2. Gulf of Aden

The beginning of continental rifting in the Gulf of Aden is only approximately known (Bosworth et al., 2005). Estimates mainly rely on the dating of sedimentary sequences, and no recent data were published. The evidence of rift initiation was summarized by Bosworth et al. (2005). Various sedimentary indications, including onshore outcrops in Yemen (Watchorn et al., 1998) and in Oman (Roger et al., 1989) and offshore wells (Hughes et al., 1991), suggest that rifting in the central and eastern Gulf of Aden began at early to mid-Oligocene, within the Rupelian, i.e., 33.9 - 27.8 Ma. Syn-rift sediments from the central Yemeni margins indicate that rift flank uplift occurred before any significant regional extension. The continental rifting climax is estimated between 20 and 18 Ma (Watchorn et al., 1998). Radiometric dating indicates that the margins became stable already in the Early Miocene (Bosworth et al., 2005), and rift-to-drift transition is interpreted to occur between ~21.1 and ~17.4 Ma (Watchorn et al., 1998). The seafloor spreading center in the Gulf of Aden is developed along most of its length and is connected to the mid-ocean ridge in the Indian Ocean through the Sheba Ridge (Gillard et al., 2021). In the central Gulf of Aden, magnetic isochrons suggest opening rates of ~27 mm/yr prior to 11 Ma, and a slowdown after 11 Ma (Fig. 4). Chron 5C (purple stripes in Fig. 3; 16.0 Ma) is present along the Gulf of Aden up to the Shukra al Sheik discontinuity (Fournier et al., 2010). This implies that the spreading center developed rapidly, perhaps instantaneously, in geological time scales, covering a distance of more than 700 km in less than 1.5 Ma.

This fast propagation ceased at the Shukra al Sheik discontinuity (Fig. 3). The youngest magnetic isochrons (2A, 2.6 Ma) are recognized up to longitude 43.9°E in the eastern Gulf of Tadjoura, ~150 km west to the Shukra al Sheik discontinuity, indicating that along this segment, the ridge propagated westward at an average rate of ~11 mm/yr, in the last 16 Ma. Within the Gulf of Tadjoura, no direct evidence of oceanic spreading was reported to our best knowledge.

4.3. Red Sea

It is not certain when continental rifting in the Red Sea began; however, sedimentary sequences suggest it postdates rifting in the Gulf of Aden by a few million years (Bosworth et al., 2005). Independent evidence suggests that rifting had begun simultaneously along the entire Red Sea at late Oligocene-Early Miocene, ~23 Ma (Plaziat et al., 1998; Szymanski et al., 2016; Stockli and Bosworth, 2018; Morag et al., 2019). Magnetic isochrons associated with seafloor spreading are only known from the southern parts of the Red Sea. However, oceanic lithosphere is probably abundant along most of the basin (Augustin et al., 2021). Chron 3 (4.2 Ma) is only present between latitudes 16° and 18°, while chrons 2A (2.6 Ma) and 2 (1.8 Ma) are present up to latitude 22° (Schettino et al., 2016). Evidence for Chron 5 (10 Ma) in the central Red Sea was recently suggested to mark the beginning of seafloor spreading (Okwokwo et al., 2022). Structural reconstructions, geodetic measurements, and magnetic anomalies suggest opening rates of ~11 mm/yr in the central parts of the basin, with an abrupt increase at ~5 Ma (Fig. 4) (Schettino et al., 2018). The southern edges of the magnetic chrons suggest that the ridge rapidly propagated southwards, with rates of ~30 mm/yr, between chrons 3 (4.2 Ma) and 2A (2.6 Ma). Since 2.6 Ma, the Red Sea ridge has not propagated southward, probably due to the decrease in angular velocity of Danakil relative to Arabia (Fig. 3 ; Schettino et al., 2018).

4.4. Main Ethiopian Rift

Results from many years of extensive fieldwork (see Corti, 2009 for review) suggest a diachronous development of the different segments of the Main Ethiopian Rift. However, there is no agreement regarding the exact timing of events and even the propagation trend of the rift. Reconstructions based on magnetic anomalies from the Southwest Indian ridge suggest an upper limit for the Nubia-Somalia separation at ~19 Ma, including large uncertainties (DeMets and Merkouriev, 2016) (Fig. 4). There are indications that rifting in East Africa started at the Turkana depression in southern Ethiopia (Varet, 2018) and propagated north to Afar (Wolfenden et al., 2004); however, this is still a matter of debate (see figs 42-44 in Corti, 2009). Radiometric dating of structural features indicates that extension commenced at ~11 Ma within the northern Main Ethiopian Rift (Wolfenden et al., 2004).

In summary, regional uplift and flood basalt volcanism in Ethiopia preceded the rifting of the Afro-Arabian rift. The rift arms developed at different times, when rifting in the eastern Gulf of Aden started during the late phases of flood basalt volcanism in Ethiopia. Rifting in the Red Sea and the Main Ethiopian Rift started in a lag of ~5-7 Ma after flood basalt volcanism.

5. Data and Methods

We used bathymetry and topography data to identify morphotectonic features. To highlight and map the architecture of the margins and axes of the rifts, we applied the Difference of Gaussians method to the topography and the bathymetry grids (Akram et al., 2017). This method allows a fast and accurate edge

detection of elevation using active spatial bandpass filtering. We applied luminance coloring to the resulting grid using the open-source image processing software Gimp.org.

To study density-related shallow crustal structures, we used the satellite altimetry-derived vertical gravity gradient (VGG) model of Sandwell et al. (2014), offering 1 arc-min resolution at offshore regions. As higher frequencies are intensified in the spectral power of the VGG, its anomalies are more source-localized and shallow-sensitive than free-air anomalies. To enhance the edges associated with the VGG, we applied a linear 11-colors colormap, further applied transparency to the VGG map, and projected it on a shaded relief (Fig. 5a).

To study deeper crustal structures and eliminate the topography effect, we used Bouguer gravity anomaly (BGA), derived from the XGM2019 gravity model (Zingerle et al., 2020), calculated with a grid step of 0.1 degrees. The XGM2019 is the most updated global gravity model of the ICGEM and is provided in terms of spherical harmonics up to 2159 degrees (Ince et al., 2019; Zingerle et al., 2020). In addition, we applied a linear 240-colors colormap to enhance BGA structures, further applied transparency to the BGA map, and projected it on a shaded relief (Fig. 5b).

To better correlate and discriminate crustal structures and rift features, we considered 1913 earthquake locations from the International Seismological Centre catalog with minimum magnitudes above 4 ML, recorded between 1964 and 2019. To better infer recent tectonic and volcanic activity, we further considered the locations of Quaternary onshore volcanoes, from the Global Volcanism Program (Smithsonian Institution) and Google Earth mapping.

6. Results

6.1. Rift margins

The most prominent morphological feature of the rift system is the escarpment along its shoulders. The escarpments mark the rift margin as they distinguish between (1) uplifted pre-rift rocks of the Arabo-Nubian shield or trap basalts sequences and (2) Quaternary arid fluvial sediments or young volcanic sequences, although several continental crustal fragments are present within the Afar Triangle. Thus, the escarpments are very distinctive in the topographical and gravity data. The edge detection analysis of topography and bathymetry data allows us to outline the rift margins (Fig. 6).

In the Red Sea, the escarpments are generally continuous with an average rift width of 440 ± 20 km (calculated perpendicular to the Red Sea axis in the study area), and a general increase in rift width from north to south (Fig. 6b). We identify two segments that mark an abrupt change in rift orientation and rift width: (1) Below latitudes 15.5° on the African margin and 18° on the Arabian margin (segment I in Fig. 6), the escarpment deviate from its general parallel to the Red Sea trend, bending towards the Afar region. The escarpment is characterized by seismic activity from that point on the African side, which is also considered the northern point of the western Afar margins (Zwaan et al., 2020a). (2) Below latitudes 12.5° on the African margin and 15° on the Arabian margin (segment II in Fig. 6), we identify another abrupt change, both in the orientation and the width of the rift. That point on the African margin is the intersection of the Tendaho-Goba'ad Discontinuity with the Western Afar Margins (Tesfaye et al., 2003). We note that these changes are noticeable and similar on the African and Arabian sides.

In the Gulf of Aden, the escarpments generally follow the trend of the basin. In the western parts, the escarpments are less straight and less continuous than those of the Red Sea and generally reflect the sinistral basin structures. This morphology is well explained by oblique rifting along the Gulf of Aden (Leroy et al., 2013). The average rift width in the study area is 470 ± 45 km (calculated rift-perpendicular), with a general eastward increase (Fig. 6b). We recognize an abrupt change in rift width along three lines (III-V in Fig. 6), which are associated with fracture zones. Along the Somalian margin, prominent sinistral offsets are recognized along lines III and V. This escarpment segment is a morphological continuation of the Tendaho-Goba'ad Discontinuity lineament, and is also prominent in the VGG map (Fig. 5a).

Although recognizable in the processed topography map, the rift shoulders are less sharp in the Main Ethiopian Rift (Fig. 6a). They are prominent in the gravity data as they are associated with VGG and BGA highs (see profile A in Fig. 9). In the Afar region, the margins show a funnel shape (Fig. 6a). The distance between the Somalian and Ethiopian escarpments is steadily and monotonically increasing from the Main Ethiopian Rift to the Tendaho-Goba'ad Discontinuity (Fig. 6b), suggesting that this segment is intact and non-disturbed by the other arms of the rift system.

In summary, the rift margins of the Red Sea and the Gulf of Aden are interrupted by the proximity to the Afar region, whereas the margins of the Main Ethiopian Rift smoothly funnel into the Afar region.

6.2. Rift axes

Along the Red Sea and the Gulf of Aden basins, the rift axes are distinctively characterized by deep and sharp bathymetric troughs, VGG lows, BGA highs, and intense seismic activity. However, with the proximity to the Afar region, the rift axes change their characteristics.

The rift axis along the Red Sea is outlined by a deep and wide axial trough that ends at latitude 14.5°, approximately 400 km from the triple junction (Fig. 7a). South of latitude 14.5°, we find geophysical evidence that the rift axis is bent, entering the Afar region at the Bay of Beylul (latitude 13.3°): (1) The VGG signature of the Red Sea axis, with highs along the walls of the axial trough and a low above the center (Fig. 7b and profile B). (2) A trail of volcanic islands follows its path (Hanish-Zukur Islands; Fig. 3), and the alignments of volcanic cones and vents on the islands are orthogonal to the trail of the islands (Mitchell and Bosworth, (in press); Gass et al., 1973). (3) A general trend of recent onshore magmatism meets this line at the Bay of Beylul (Fig. 3). However, major fault sets are not observed in the onshore area of Beylul (Rime et al., 2023). (4) This line best fits GPS-based rigid block model (Viltres et al., 2020), and is supported by the fact that the rotation of Danakil relative to Arabia stopped around l ~0.3 Ma (following Schettino et al., 2018 and personal communication). In addition to this bent segment, a typical gravity signature of the rift axis with a central BGA high and VGG picks to its side, is also recognized along the connection of the Red Sea with the Gulf of Aden at Bab al Mandab Strait (latitudes 13.2° to 12.3°; Fig. 7 profile CC'). Nevertheless, this segment is not an active rift axis as no earthquake, volcanic or bathymetrical expression is associated with it, however, diluted activity is also understood by the low and oblique velocity of Arabia in this area (Fig. 3).

In the Gulf of Aden, there is also a distinct change in the rift axis characteristics, approximately 400 km from the triple junction (Fig. 8). Up to the Shukra al Sheik discontinuity, the Gulf of Aden is a deep basin, reaching depths of more than 1,000 m only a few kilometers from the shore, and has a fragmented axial trough, offset by oblique left-lateral transform faults. West to the Shukra al Sheik discontinuity, the basin is shallow, and the axial trough is very distinct, characterized by deep and sharp morphology. This ~400 km long curved axis segment impales the Afar triangle at the Gulf of Tadjoura (Djibouti). This axial segment

has a distinct gravity signature and is characterized by intensive seismic activity, perhaps the most intensive in the rift system, with over 1,000 recorded events with magnitudes above 4ML (ISC catalog).

In the Main Ethiopian Rift, there are no abrupt changes in the characteristics of the rift valley with the proximity to the Afar triangle (Fig. 9). Instead, the rift valley goes through an elevated dome peaking approximately 400 km from the triple junction (Fig. 9a). The along-strike profile (profile B in Fig. 9) shows that the rift valley reaches altitudes of more than 2,000 m and is associated with a BGA low.

In the Afar triangle, the morphology indicates several axial segments, which are also distinctive in the VGG map (Fig. 10). We recognize axial trends in two distinguished and geographically separated regions: (1) southwest to the Tendaho-Goba'ad Discontinuity, a NE trending valley continues the trend of the Main Ethiopian Rift, characterized by distinct central volcanoes along with an axial depression. (2) Northeast to the Tendaho-Goba'ad Discontinuity, typical rift axial morphologies, composed of NW trending short segments along volcanic ranges, are abundant over a 200 km wide zone. Hence, the Afar depression is divided into two morphological regions, in terms of axial trends, parallel to the Main Ethiopian Rift trending region and the Red Sea trending region.

In summary, with the proximity to the Afar depression, the rift axes of the Red Sea and the Gulf Aden are not persistent and drastically change their characteristics ~400 km from the triple junction. In contrast, the axis of the Main Ethiopian Rift is consistent, keeping its trend and characteristics up to the triple junction point.

7. Discussion

7.1. The architecture of the intersection region

The Afar triangle is the intersection region of three rift arms: the Gulf of Aden, the Red Sea, and the Main Ethiopian Rift. Far from the intersection region, the axes and margins of these rifts follow a general parallel trend, suggesting that rigid plate tectonics of the Nubian, Arabian, and Somalian plates controlled their structural development (Garfunkel and Beyth, 2006; Reilinger et al., 2006; Reilinger and McClusky, 2011; Schettino et al., 2018). Within the Afar triangle, southwest to the Tendaho-Goba'ad discontinuity, the rift margins are continuous and smooth, and the axial volcanic range generally continues the trend of the axial valley of the Main Ethiopian Rift, reflecting a sub-perpendicular extension in accordance with the Nubia – Somalia kinematics, and thus, could be regarded as a rigid plate boundary. However, the architecture of the intersection region northeast of the Tendaho-Goba'ad discontinuity is more complex and is not simply resolved by rigid plate kinematics (Garfunkel and Beyth, 2006).

Fig. 11 summarizes the rift margins and the axial segments mapped in this study. The rift axes of the Gulf of Aden and the Red Sea abruptly change their characteristics, particularly their trends, with the proximity to the Afar region. Around ~400 km from the triple junction, the Gulf of Aden and the Red Sea axes deviate from their basin parallel trend, bending towards the third and younger arm of the Main Ethiopian Rift. Within the Afar triangle, northeast of the Tendaho-Goba'ad discontinuity, the margins are fragmented, and there are multiple, short, and sub-parallel axial segments.

In our study, the term "axial segments" inferred is not simply correlated with rift axes, as the geology in this region is quite complex, including several fault and transfer zones, and, exposing pre-rift rock sequences. However, the axial segments mapped in this study in the continental area northeast to the

Tendaho-Goba'ad discontinuity is somewhat correlative with rift axes that had been suggested based on field observations (e.g., Rime et al., 2023). Axial segments are generally sub-parallel to the Red Sea axis (Zwaan et al., 2020b), which led authors to suggest that this region reflects an evolving discontinuity of the oceanic spreading center in the Red Sea (e.g. Tazieff et al., 1972; Bosworth et al., 2005). Although several focal solutions indicated dextral strike-slip motions in this area, we don't find other evidence for a typical first-order transform connection between the ridge in the Red Sea and the continuation of the northern Afar axial segments, offshore Gulf of Zula. Magnetic stripes in the Red Sea are observed at more than 200 km south of the Gulf of Zula region (Fig. 12), and the volcanic ridge in the southern Red Sea is very active (Eyles et al., 2018). Although earthquake clusters at latitude 16.5° indicate strike-slip solutions, supporting a structural connection to the Red Sea axis, these are abundant throughout the study area (Hofstetter and Beyth, 2003). Alternatively, it is possible to regard the jump between the Red Sea ridge to the axial segments in northeastern Afar as a non-transform discontinuity. However, second-order discontinuities are usually characterized by <30 km offsets, and here the jump is ~200 km (Macdonald et al., 1984; Carbotte et al., 2016). Thus, we find no circumstantial evidence to regard the axial volcanism in the Afar depression as part of the development of the Red Sea spreading center. This conclusion agrees with the study of Rime et al. (2023), which discusses the geological evidence from Afar.

Our analysis highlights that the area northeast to the Tendaho-Goba'ad discontinuity is characterized by diffuse deformation, reflecting a rugged connection of the Red Sea and the Gulf of Aden arms to the Main Ethiopian Rift. Kinematic studies support this view, indicating that microplate rotations and diffuse boundaries significantly influence the structural development of this region. A recent model based on GPS observations (Viltres et al., 2020) reveals a diffuse character of the Danakil - Nubia boundary with inter-rifting deformation over more than 100 km wide zone. The Danakil microplate extends to the Hanish-Zukur Islands at its southern edge (~13.8°N) with no precise/sharp boundary. The Danakil microplate is rotating counterclockwise (Manighetti et al., 2001), while the Ali-Sabieh block, south of the Gulf of Tadjoura, is rotating clockwise (Audin et al., 2004), described as a "saloon-doors" mode of opening (Kidane, 2016).

Observations and analog models indicate that strain in Afar is localized in distinct rift segments, which are spread within a broad zone of interaction of the associated plates (Keir et al., 2011; Pagli et al., 2014, 2018; Doubre et al., 2017; Maestrelli et al., 2022). Hence, the architecture of the intersection region of the rift arms discloses a ~150,000 km^2 complex region, in which diffuse boundaries and microplate rotations link the three rift arms (Fig. 11). Accordingly, a genuinely single triple junction point, in the sense of a three-rift arms intersection point, cannot be specified for this system, and multiple triple junctions could be considered (e.g., see tectonic models in Viltres et al., 2020). The difficulty of defining sharp plate boundaries within Afar was discussed in many works (e.g., Barrberi and Varet, 1977 and references therein). Nevertheless, we agree that the intersection point of the Ethiopian rift valley and the Tendaho-Goba'ad Discontinuity could be regarded as the 'main' junction point of the rift system, as the deformation characteristics are most distinctively changed there (Tesfaye et al., 2003).

7.2. Spatial constraints in the development of the plume-rift system

The architecture of the Afar region allows us to draw two spatial constraints in the development of the plume-rift system:

(1) The first is the connection of the Main Ethiopian Rift to the Gulf of Aden - Red Sea rifts by a northeastward propagation. Since the divergence between Nubia-Somalia is sub-vertical to the strike of the northern Main Ethiopian Rift, resolving its propagation direction is quite intangible and conversed

(Tesfaye et al., 2003; Wolfenden et al., 2004; Bonini et al., 2005; Keranen and Klemperer, 2008; Abebe et al., 2010).The margins of southeast Afar show symmetric, continuous, and smooth curved trends, from the elevated regions of the Main Ethiopian Rift to the Tendaho-Goba'ad Discontinuity (Fig. 6). With respect to the northeastward trend of the Main Ethiopian rift, the Somalian margin is curved clockwise, like the Ali-Sabieh sense of rotation (Kidane, 2016), whereas, the Ethiopian margin is curved counterclockwise, like the Danakil sense of rotation (Schult, 1974). This architecture could be understood in terms of fracture mechanics by reorientating a propagating fracture near a pre-existing fracture. Strain analysis indicates that a propagating fracture would curve parallel to the pre-existing fracture under a tensional stress field due to free surface boundary conditions induced by the open pre-existing fracture (Dyer, 1988). Thus, this macro scale architecture may express a smooth linkage of the Main Ethiopian Rift to the pre-existing Gulf of Aden-Red Sea rifts by a northeastward propagation. Hence, this implies that a triple junction formed at a late stage, when all three arms were already significantly developed. This conclusion agrees with structural geochronology within the northern Main Ethiopian Rift, showing that extension in the northern Main Ethiopian rift commenced at 11 Ma (Wolfenden et al., 2004).

(2) The second spatial constraint is abandoning an early tectonic connection between the Red Sea and the Gulf of Aden through the Bab al-Mandab Strait. As the VGG and neovolcanic activity indicate that the Red Sea axis currently enters Afar at the Bay of Beylul (see section 6.2), we find arguments for an earlier tectonic connection between the Red Sea and the Gulf of Aden through Bab al-Mandab Strait: (i) Below latitude 13.2° and up to the connection to the Gulf of Aden (at latitude 12.3°), the gravity data shows typical rift axis characteristics, with BGA high and VGG picks to its side (Fig. 7 and Fig. 8; see section 6.2). (ii) The submarine channel north to the Hanish Island (latitude 13.4°) shows no association with modern water currents and may be explained by subsurface rift structures (Mitchell and Sofianos, 2018). (iii) This is the straight continuation of the trend of the Red Sea axis, along which the basins are curtly connected (Fig. 1). Thus, it is reasonable that it was also the tectonic connection in the early stages of rift development. Likewise, reconstructions suggest that the Danakil microplate started to rotate in the Middle Miocene (~10 Ma), when Arabia was already separated from Africa (Collet et al., 2000; Schettino et al., 2016; Rime et al., 2023). Those reconstructions show that until that time, the divergence was focused along the seaway at the southernmost Red Sea. This suggests that the present deviation from the basin parallel trend of the rift axes at the tip of the Gulf of Aden and the Red Sea marks a tectonic reorganization in this region.

Adopting the fracture propagation analog postulated here for the northeastward propagation of the Main Ethiopian Rift, it follows that the abandonment of the tectonic connection between the Red Sea and the Gulf of Aden happens as a response to the new stress conditions in Afar. Rime et al. (2023) suggest that the deposition of lacustrine sediments in Afar (Chorora Fm) marks the development of the Main Ethiopian Rift in Afar. They point out that these sediments were deposited roughly at the same time to the individualization of the Danakil Block, and thus to the reduction in the tectonic activity of the southernmost Red Sea rift.

These two spatial constraints indicate that the onset of the triple junction happened at a late stage when the three rift arms were already developed and the Red Sea was tectonically connected to the Gulf of Aden, far (~250 km) from the present-day triple junction (Fig. 13). The onset of the triple junction marks a tectonic reorganization and microplate formation. As a result, the Gulf of Aden and the Red Sea arms are not smoothly connected to the Main Ethiopian Rift, and a vast area of diffuse and complex deformation developed within the intersection region.

7.3. Mechanisms for plume-rift association

The temporal constraints regarding the development of the plume-rift features, summarized in section 4, together with the two spatial constraints inferred in this study, allow us to examine the causal relationship between the activity of the Afar plume and rifting. Our insights suggest that neither 'active' nor 'passive' rifting mechanisms are solely consistent with the observation. Passive rifting models fail to explain the plume-rift association mainly because the flood basalt volcanism cannot be attributed to passively rising asthenospheric mantle beneath a stretched and thinned lithosphere, as dynamic uplift in Ethiopia was shown to be a long-lasting process, prior to flood basalt volcanism (Sembroni et al., 2016). Hence, rifting and associated subsidence are subsequent to flood basalt volcanism (Fig. 4). The estimations of ~1 km elevation before flood basalts (Fig. 4) coincide with active plume-head predictions (Campbell and Griffiths, 1990). Moreover, the passive model does not explain why a triple junction is located within the flood basalts area, as rifting in the Red Sea and Gulf of Aden are at an oblique angle to the former sutures (Buiter and Torsvik, 2014).

On the other hand, active models are not in line with the progressive development of the rifts, mainly because the flood basalts region cannot be considered a center or a nucleus, from which rift arms spread, as expected in an actively generated triple junction. Numerous studies noted that the tectonic development of the Afar region is not compatible with a simplified model of rift arms that simultaneously spread away from a triple junction (see Section 5.2 in Rime et al., 2023 for a review). The inset of a triple junction was the last feature to develop in the system, by the propagation of the Main Ethiopian Rift towards Afar, followed by a tectonic reorganization including the abandonment of a former tectonic connection between the Red Sea and the Gulf of Aden. By this time, the rift arms had already developed, and the break-up had already been accomplished between Africa and Arabia. This tectonic reorganization cannot be attributed to the development of gravitational potential by the plume head (Hill, 1991), as it occurred millions of years after flood basalts magmatism. That rules out the possibility that the arrival of the Afar plume generated the onset of the triple junction, as more than 20 Ma separate these events and the rift arms did not spread from the plume region.

We propose a scenario in which rifting was triggered by a plume-induced plate rotation (Fig. 2c). Numerical simulations suggest that horizontal asthenospheric flows due to the arrival of a plume head at the base of the lithosphere induce a plume-push force that can accelerate plates by several cm yr^{-1} (van Hinsbergen et al., 2011, 2021; Pusok and Stegman, 2020). In this scenario, flood basalt volcanism would be synchronous to an abrupt plate speed-up and thus to new remote stress conditions. In the case of the Indian plate, at least two episodes of massive flood basalt volcanism, Morondava LIP (~94 Ma) and Deccan traps (67 Ma), are associated with plume-derived plate acceleration, and a drastic change in the tectonic framework (van Hinsbergen et al., 2011, 2021; Cande and Stegman, 2011; Pusok and Stegman, 2020). Further, torque balance modeling suggests that horizontal plume-push can force a significant plate rotation and, consequently, initiate new plate boundaries (van Hinsbergen et al., 2021).

In the Afro-Arabian rift, indeed new plate boundaries formed after the arrival of the large Afar plume and a significant plate rotation of Arabia around a nearby pole characterizes the Arabian continent (Joffe and Garfunkel, 1987; Viltres et al., 2022). Magnetic anomalies and structural reconstructions suggest that the rotation around a nearby pole already characterized Arabia since the Oligocene (Fournier et al., 2010; Schettino et al., 2018). Additionally, the beginning of intensive volcanism in the north-western Arabian plate (Harrat Ash Shaam) at Late Oligocene (Ilani et al., 2001), reflects a change in mantle-crust interaction and intracontinental extension within the Arabian plate, adjacent to the arrival of Afar plume (Garfunkel,

1989). In the Harrat Ash Shaam volcanic field, diking directions from Miocene to recent ages record the rotation of Arabia (Giannerini et al., 1988), suggesting that already during the first stages of volcanism the Arabian plate was rotating around a nearby pole.

The arrival of the Afar plume was also accompanied by a slowdown of Africa (Le Pichon and Gaulier, 1988). By this time, Africa collided with Eurasia in the west, explaining its slowdown (Jolivet and Faccenna, 2000) and increased intraplate volcanism (Burke, 1996). However, this collision of Africa and Eurasia cannot simply resolve the change in the rotation of Arabia as the Arabian continent collided with Eurasia not earlier than ~18 Ma (Su and Zhou, 2020), although some authors suggested that asymmetrical along-trench entrance of continental material could lead to an intraplate extension similar to those that generated the Africa-Arabia break-up (Bellahsen et al., 2003). Faccenna et al. (2013) already showed that plume-push from the Afar area resolves the present-day plate kinematics in the Middle East, particularly the anti-clockwise toroidal pattern of the Arabia–Anatolia–Aegean system. The importance of active upwelling in Afar to lateral mantle flow below Arabia is also illustrated by shear-wave splitting, indicating a general N-S anisotropy in the mantle (Qaysi et al., 2018). Stamps et al. (2014) calculated the current driving forces for the Nubia-Somalia divergence and found that gravitational potential energy is the most significant force, stronger by an order of magnitude than forces from basal shear tractions of mantle convection. They point out that the gravitational potential energy is sufficient to sustain present-day rifting in East Africa but not to initiate rupture of continental lithosphere. In the case of the Arabian plate, basal shear tractions are expected to be higher due to the orientation of northward-directed mantle flow (Faccenna et al., 2013).

If the Afar plume induced the rotation of Arabia around a nearby pole, then it is understood how the Gulf of Aden and the Red Sea rifts developed after a regional uplift and flood basalt volcanism but still geometrically developed by the new regional stress field and structural inheritance (Autin et al., 2013; Bosworth and Stockli, 2016). It also explains why the trace of the rifts intersect within the plume region as the lithosphere in this region was weakened by the hot plume material (François et al., 2018). Finally, it explains the delayed development of the Main Ethiopian Rift and the late onset of the Afar triple junction by its northwestward propagation, as these were controlled by the slower kinematics of the Somalian plate rather than dynamic forces. In this manner, ‘active’ and ‘passive’ mechanisms are coupled and have positive feedback, allowing a close occurrence of flood basalt volcanism and continental break-up, alongside a passive style of rifting.

8. Summary and Conclusions

We reviewed the geologic setting of the Afro-Arabian rift, in which vast regions of flood basalts and ongoing continental break-up are superimposed, aiming to infer a causal relationship between the activity of the deep-seated Afar plume and crustal break-up. We explored the intersection region where the Gulf of Aden, the Red Sea, and the Main Ethiopian Rift form an R-R-R triple junction, separating the large Cenozoic plume-related flood basalt series in Ethiopia and Yemen. We provide a new synthesis and interpretation of modern geophysical datasets, including topography, bathymetry, gravity, magnetic anomalies, earthquakes, and volcano distribution, to map the margins and axes of the rift arms.

We highlight key differences in the terminations of the Gulf of Aden and the Red Sea arms, which are rough and irregular, versus the symmetric, continuous, and smooth architecture of the Main Ethiopian Rift. The architecture of the intersection regions allows us to infer two tempo-spatial constraints in the

development of the rifts: (1) the connection of the Main Ethiopian Rift to the Gulf of Aden and to the Red Sea by its northeastward propagation, and, (2) the abandonment of an early tectonic connection between the Red Sea and the Gulf of Aden. These suggest a progressive development of the intersection area, including a broad region of diffuse deformation and recent tectonic reorganization. The onset of the triple junction was the last feature to develop in the plume-rift system after all rift arms were sufficiently developed and the break-up was accomplished.

This progressive development does not align with the classic active rifting model, which predicts a plume-generated triple junction at the locus of the rift, from which the rifts develop. Nevertheless, the classic passive rifting model fails to explain the chronological evidence, as flood basalts probably erupted on elevated topography before rifting started. We discuss a scenario of plume-induced plate rotation in which the arrival of the Afar plume triggered the rotation of Arabia around a nearby pole, and demonstrate that the rotation of Arabia around a nearby pole characterizes the system since the Oligocene. We suggest that this scenario better explains the progressive development of the plume-rift system in the Afro-Arabian rift.

9. Data availability

The bathymetry and topography data used in this study was retrieved from GEBCO Compilation Group (2021), available at https://www.gebco.net/data_and_products/gridded_bathymetry_data/#area.

The VGG data used in this study is available at https://topex.ucsd.edu/grav_outreach/.

The BGA data used in this study is available at http://icgem.gfz-potsdam.de/calcgrid; model XGM2019e-2159, 'gravity_anomaly_bg'.

Earthquake data was retrieved from the International Seismological Centre (2020), On-line Bulletin, https://doi.org/10.31905/D808B830.

Quaternary onshore volcano locations were retrieved from the Global Volcanism Program, Smithsonian Institution, available at https://volcano.si.edu/volcanolist_holocene.cfm.

Magnetic anomalies data is available at https://figshare.com/articles/dataset/Transcurrent_Regimes_During_Rotational_Rifting_New_Insights_from_Magnetic_Anomalies_in_the_Red_Sea/14743272.

10. Author contribution

RI carried out the study and wrote and revised the original draft of this paper. PH and NA provided conceptual assistance, helped in writing and reviewed the manuscript. JE mentored the study, took care of administration, and reviewed the manuscript.

11. Competing interests

The contact author has declared that neither of the authors has any competing interests.

12. Acknowledgments

This work was supported by the grants from Minerva Fellowship to R. I. We thank Neil Mitchell and Valentin Rime for their helpful discussion throughout the open discussion process. We wish to thank Antonio Schettino and Derek Keir for their review which helped improving the manuscript.

13. Figure captions

Fig. 1. Elevation map of the study area, showing the general plate tectonic configuration (from USGS and from Viltres et al. (2020) in the Afar region) and Cenozoic volcanics (modified from Varet, 1978; Davison et al., 1994; Beyene and Abdelsalam, 2005; Bosworth and Stockli, 2016) Black arrows indicate GPS velocities in respect to Nubia (modified from Reilinger et al., 2006).

Fig. 2. Schematic mechanisms for plume-rift association in the Afro-Arabian rift. (a) Active mechanism, in which rifting results from the actively rising head of the Afar plume. In this mechanism impinging and eroding the base of the lithosphere prompt uplift and decompression melting and flood basalts volcanism. These introduce internal extensional forces and ultimately lead to break-up. (b) Passive mechanism, in which rifting is initiated solely by the remote stresses, regardless of underlying Afar plume. In this mechanism the production of massive volcanism is allowed when the thinned and stretched lithosphere is underlaid by the thermal anomaly in the mantle. Flood basalts volcanism is generated by passively rising decompression melting of hot asthenospheric mantle. (c) Plume-induced plate rotation, in which lateral forces, induced by the arrival of the Afar plume head, add up to the remote stresses to change the plate kinematics. In this mechanism flood basalts volcanism is actively controlled, however, rifting is triggered by the new plate kinematics.

Fig. 3. Map of the Afar region showing magnetic isochrons (modified from Fournier et al., 2010; Bridges et al., 2012; Schettino et al., 2016), earthquake locations (from ISC catalog), Holocene onshore volcano locations (from GVP catalog and Viltres et al. (2020)) and recent volcanism (modified from Keir et al., 2013).

Fig. 4. Elevation of the Ethiopian–Yemen plateau (after Sembroni et al., 2016; Faccenna et al., 2019), volcanic episodes and openinng rates of the rift arms (modified from Fournier et al., 2010; DeMets and Merkouriev, 2016; Schettino et al., 2018). Dashed lines indicate estimations from geological observations and soild lines from magnetic isochrons.

Fig. 5. Gravity data of the Afar region. (a) Vertical gravity gradient from Sandwell et al. (2014). Bouguer anomaly model from ICGEM, XGM2019e (Zingerle et al., 2020).

Fig. 6. (a) Difference of Gaussians applied to topography and bathymetry showing rift margins (black lines). White dashed lines indicate peaks in rift width. TGD is the Tendaho-Goba'ad Discontinuity. SSD is the Shukra al Sheik discontinuity. Black dots indicate earthquake locations (ISC catalog). (b) Rift widths, calculated in rift-perpendicular directions.

Fig. 7. Bathymetry (a), vertical gravity gradient (b) and Bouguer anomaly (c) in the southern Red Sea. Black dots indicate earthquake locations (ISC catalog). (d) Profiles across rift axis.

Fig. 8. Bathymetry (a), vertical gravity gradient (b) and Bouguer anomaly (c) in the Western Gulf of Aden. Black dots indicate earthquake locations (ISC catalog). (d) Profiles across rift axis.

Fig. 9. Topography (a), vertical gravity gradient (b) and Bouguer anomaly (c) in the northern Main Ethiopian Rift. Black dots indicate earthquake locations (ISC catalog). (d) Profiles across (AA') and along (BB') the rift valley.

Fig. 10. Topography (a), vertical gravity gradient (b) and Bouguer anomaly (c) in the Afar triangle. Black dots indicate earthquake locations (ISC catalog). TGD is the Tendaho-Goba'ad Discontinuity. (d) Profiles SW (AA') and NE (BB') to the TGD.

Fig. 11. Rift margins (solid white lines) and axial segments (long dashed black lines) in the Afar region. Black dots indicate earthquake locations (ISC catalog). TGD is the Tendaho-Goba'ad Discontinuity.

Fig. 12. Tilt-angle derivative map of magnetic anomalies, projected on a shaded relief after Issachar et al. (2022). Purple colures represent positive angles and green colors represent negative angles. White dashed lines indicate magnetic stripes (Schettino et al., 2016).

Fig. 13. Synthesis of the progressive development of the rift intersections.

14. References

Abebe, T., Balestrieri, M.L., and Bigazzi, G., 2010, The Central Main Ethiopian Rift is younger than 8 Ma: confirmation through apatite fission-track thermochronology:, doi:10.1111/j.1365-3121.2010.00968.x.

Akram, F., Garcia, M.A., and Puig, D., 2017, Active contours driven by difference of Gaussians: Scientific Reports, v. 7, p. 1–15, doi:10.1038/s41598-017-14502-w.

Anderson, D.L., 2005, Large Igneous Provinces, Delamination, and Fertile Mantle: Elements, v. 1, p. 271–275, doi:10.2113/gselements.1.5.271.

Anderson, D.L., 1994, The sublithospheric mantle as the source of continental flood basalts; the case against the continental lithosphere and plume head reservoirs: Earth and Planetary Science Letters, v. 123, p. 269–280, doi:https://doi.org/10.1016/0012-821X(94)90273-9.

Audin, L., Quidelleur, X., Coulié, E., Courtillot, V., Gilder, S., Manighetti, I., Gillot, P.Y., Tapponnier, P., and Kidane, T., 2004, Palaeomagnetism and K-Ar and 40 Ar/39 Ar ages in the Ali Sabieh area (Republic of Djibouti and Ethiopia): Constraints on the mechanism of Aden ridge propagation into southeastern Afar during the last 10 Myr: Geophysical Journal International, v. 158, p. 327–345, doi:10.1111/j.1365-246X.2004.02286.x.

Augustin, N., van der Zwan, F.M., Devey, C.W., and Brandsdóttir, B., 2021, 13 million years of seafloor spreading throughout the Red Sea Basin: Nature Communications, v. 12, p. 1–10, doi:10.1038/s41467-021-22586-2.

Autin, J., Bellahsen, N., Leroy, S., Husson, L., Beslier, M.O., and d'Acremont, E., 2013, The role of structural inheritance in oblique rifting: Insights from analogue models and application to the Gulf of Aden: Tectonophysics, v. 607, p. 51–64, doi:10.1016/J.TECTO.2013.05.041.

Barrberi, F., and Varet, J., 1977, Volcanism of Afar: Small-scale plate tectonics implications: GSA Bulletin, v. 88, p. 1251–1266, doi:10.1130/0016-7606(1977)88<1251:VOASPT>2.0.CO;2.

Bellahsen, N., Faccenna, C., Funiciello, F., Daniel, J.M., and Jolivet, L., 2003, Why did Arabia separate from Africa? Insights from 3-D laboratory experiments: Earth and Planetary Science Letters, v. 216, p. 365–

381, doi:10.1016/S0012-821X(03)00516-8.

Bellahsen, N., Husson, L., Autin, J., Leroy, S., and D'Acremont, E., 2013, The effect of thermal weakening and buoyancy forces on rift localization: Field evidences from the Gulf of Aden oblique rifting: Tectonophysics, v. 607, p. 80–97, doi:10.1016/j.tecto.2013.05.042.

Bellieni, G., Visentin, E.J., Zanettin, B., Piccirillo, E.M., Radicati di Brozolo, F., and Rita, F., 1981, Oligocene transitional tholeiitic magmatism in Northern turkana (Kenya): Comparison with the Coeval Ethiopian volcanism: Bulletin Volcanologique, v. 44, p. 411–427, doi:10.1007/BF02600573.

Beyene, A., and Abdelsalam, M.G., 2005, Tectonics of the Afar Depression: A review and synthesis: Journal of African Earth Sciences, v. 41, p. 41–59, doi:10.1016/j.jafrearsci.2005.03.003.

Bonini, M., Corti, G., Innocenti, F., Manetti, P., Mazzarini, F., Abebe, T., and Pecskay, Z., 2005, Evolution of the Main Ethiopian Rift in the frame of Afar and Kenya rifts propagation: v. 24, doi:10.1029/2004TC001680.

Bosworth, W., 2015, Geological evolution of the Red Sea: historical background, review, and synthesis, *in* In The Red Sea, Springer, Berlin, Heidelberg, p. 45–78, doi:10.1007/978-3-662-45201-1.

Bosworth, W., Huchon, P., and McClay, K., 2005, The Red Sea and Gulf of Aden Basins: Journal of African Earth Sciences, v. 43, p. 334–378, doi:10.1016/j.jafrearsci.2005.07.020.

Bosworth, W., and Stockli, D.F., 2016, Early magmatism in the greater Red Sea rift: Timing and significance: Canadian Journal of Earth Sciences, v. 53, p. 1158–1176, doi:10.1139/cjes-2016-0019.

Bridges, D.L., Mickus, K., Gao, S.S., Abdelsalam, M.G., and Alemu, A., 2012, Magnetic stripes of a transitional continental rift in Afar: Geology, v. 40, p. 203–206, doi:10.1130/G32697.1.

Bryan, S.E., and Ferrari, L., 2013, Large igneous provinces and silicic large igneous provinces: Progress in our understanding over the last 25 years: GSA Bulletin, v. 125, p. 1053–1078, doi:10.1130/B30820.1.

Buiter, S.J.H., and Torsvik, T.H., 2014, A review of Wilson Cycle plate margins: A role for mantle plumes in continental break-up along sutures? Gondwana Research, v. 26, p. 627–653, doi:10.1016/J.GR.2014.02.007.

Burke, K., 1996, The African Plate: South African Journal of Geology, v. 99, p. 341–409, doi:10.10520/EJC-942801F20.

Burke, K., and Dewey, J.F., 1973, Plume-generated triple junctions: key indicators in applying plate tectonics to old rocks: The Journal of Geology, v. 81, p. 406–433, doi:https://doi.org/10.1086/627882.

Campbell, I.H., and Griffiths, R.W., 1990, Implications of mantle plume structure for the evolution of flood basalts: Earth and Planetary Science Letters, v. 99, p. 79–93, doi:10.1016/0012-821X(90)90072-6.

Cande, S.C., and Stegman, D.R., 2011, Indian and African plate motions driven by the push force of the Réunion plume head: Nature, v. 475, p. 47–52, doi:10.1038/nature10174.

Carbotte, S.M., Smith, D.K., Cannat, M., and Klein, E.M., 2016, Tectonic and magmatic segmentation of the Global Ocean Ridge System: A synthesis of observations, *in* Geological Society Special Publication, Geological Society of London, v. 420, p. 249–295, doi:10.1144/SP420.5.

Chatterjee, S., Goswami, A., and Scotese, C.R., 2013, The longest voyage: Tectonic, magmatic, and paleoclimatic evolution of the Indian plate during its northward flight from Gondwana to Asia: Gondwana Research, v. 23, p. 238–267, doi:10.1016/j.gr.2012.07.001.

Chorowicz, J., 2005, The East African rift system: Journal of African Earth Sciences, v. 43, p. 379–410,

671 doi:10.1016/j.jafrearsci.2005.07.019.

672 Collet, B., Taud, H., Parrot, J.F., Bonavia, F., and Chorowicz, J., 2000, A new kinematic approach for the
673 Danakil block using a Digital Elevation Model representation: Tectonophysics, v. 316, p. 343–357,
674 doi:10.1016/S0040-1951(99)00263-2.

675 Corti, G., 2009, Continental rift evolution: From rift initiation to incipient break-up in the Main Ethiopian
676 Rift, East Africa: Earth-Science Reviews, v. 96, p. 1–53, doi:10.1016/j.earscirev.2009.06.005.

677 Coulié, E., Quidelleur, X., Courtillot, V., Lefèvre, J.C., and Chiesa, S., 2003, Comparative K-Ar and Ar/Ar
678 dating of Ethiopian and Yemenite Oligocene volcanism: Implications for timing and duration of the
679 Ethiopian traps: Earth and Planetary Science Letters, v. 206, p. 477–492, doi:10.1016/S0012-
680 821X(02)01089-0.

681 Courtillot, V., Jaupart, C., Manighetti, I., Tapponnier, P., and Besse, J., 1999, On causal links between flood
682 basalts and continental breakup: Earth and Planetary Science Letters, v. 166, p. 177–195,
683 doi:10.1016/S0012-821X(98)00282-9.

684 Davison, I. et al., 1994, Geological evolution of the southeastern Red Sea Rift margin, Republic of Yemen:
685 Geological Society of America Bulletin, v. 106, p. 1474–1493, doi:10.1130/0016-
686 7606(1994)106<1474:GEOTSR>2.3.CO;2.

687 DeMets, C., and Merkouriev, S., 2016, High-resolution estimates of Nubia-Somalia plate motion since 20
688 Ma from reconstructions of the Southwest Indian Ridge, Red Sea and Gulf of Aden: Geophysical
689 Journal International, v. 207, p. 317–332, doi:10.1093/gji/ggw276.

690 Doubre, C. et al., 2017, Current deformation in Central Afar and triple junction kinematics deduced from
691 GPS and InSAR measurements: Geophysical Journal International, v. 208, p. 936–953,
692 doi:10.1093/gji/ggw434.

693 Duclaux, G., Huismans, R.S., and May, D.A., 2020, Rotation, narrowing, and preferential reactivation of
694 brittle structures during oblique rifting: Earth and Planetary Science Letters, v. 531, p. 115952,
695 doi:10.1016/j.epsl.2019.115952.

696 Dyer, R., 1988, Using joint interactions to estimate paleostress ratios: Journal of Structural Geology, v. 10,
697 p. 685–699, doi:10.1016/0191-8141(88)90076-4.

698 Ebinger, C.J., Keir, D., Bastow, I.D., Whaler, K., Hammond, J.O.S., Ayele, A., Miller, M.S., Tiberi, C., and
699 Hautot, S., 2017, Crustal Structure of Active Deformation Zones in Africa: Implications for Global
700 Crustal Processes: Tectonics, v. 36, p. 3298–3332, doi:https://doi.org/10.1002/2017TC004526.

701 Ernst, R.E., 2014, Large igneous provinces: Cambridge University Press.

702 Eyles, J.H.W., Illsley-Kemp, F., Keir, D., Ruch, J., and Jónsson, S., 2018, Seismicity Associated With the
703 Formation of a New Island in the Southern Red Sea: Frontiers in Earth Science, v. 6, p. 1–10,
704 doi:10.3389/feart.2018.00141.

705 Faccenna, C., Becker, T.W., Jolivet, L., and Keskin, M., 2013, Mantle convection in the Middle East:
706 Reconciling Afar upwelling, Arabia indentation and Aegean trench rollback: Earth and Planetary
707 Science Letters, v. 375, p. 254–269, doi:10.1016/J.EPSL.2013.05.043.

708 Faccenna, C., Glišović, P., Forte, A., Becker, T.W., Garzanti, E., Sembroni, A., and Gvirtzman, Z., 2019, Role
709 of dynamic topography in sustaining the Nile River over 30 million years: Nature Geoscience, v. 12,
710 p. 1012–1017, doi:10.1038/s41561-019-0472-x.

711 Forsyth, D., and Uyeda, S., 1975, On the relative importance of the driving forces of plate motion:
712 Geophysical Journal International, v. 43, p. 163–200.

Fournier, M. et al., 2010, Arabia-Somalia plate kinematics, evolution of the Aden-OwenCarlsberg triple junction, and opening of the Gulf of Aden: Journal of Geophysical Research: Solid Earth, v. 115, p. 1–24, doi:10.1029/2008JB006257.

François, T., Koptev, A., Cloetingh, S., Burov, E., and Gerya, T., 2018, Plume-lithosphere interactions in rifted margin tectonic settings: Inferences from thermo-mechanical modelling: Tectonophysics, v. 746, p. 138–154, doi:10.1016/j.tecto.2017.11.027.

Frizon De Lamotte, D., Fourdan, B., Leleu, S., Leparmentier, F., and De Clarens, P., 2015, Style of rifting and the stages of Pangea breakup: Tectonics, v. 34, p. 1009–1029, doi:10.1002/2014TC003760.

Fromm, T., Planert, L., Jokat, W., Ryberg, T., Behrmann, J.H., Weber, M.H., and Haberland, C., 2015, South Atlantic opening: A plume-induced breakup? Geology, v. 43, p. 931–934, doi:10.1130/G36936.1.

Garfunkel, Z., 1989, Tectonic setting of phaneroozoic magmatism in Israel: Israel journal of earth-sciences, v. 38, p. 51–74.

Garfunkel, Z., and Beyth, M., 2006, Constraints on the structural development of Afar imposed by the kinematics of the major surrounding plates: Geological Society Special Publication, v. 259, p. 23–42, doi:10.1144/GSL.SP.2006.259.01.04.

Gass, I.G., Mallick, D.I.J., and Cos, K.G., 1973, Volcanic islands of the Red Sea: Journal of the Geological Society, v. 129, p. 275–309, doi:10.1144/gsjgs.129.3.0275.

GEBCO Compilation Group, 2021, The GEBCO_2019 Grid: a continuous terrain model of the global oceans and land:, doi:10.5285/c6612cbe-50b3-0cff-e053-6c86abc09f8f.

Geoffroy, L., 2005, Volcanic passive margins: Comptes Rendus Geoscience, v. 337, p. 1395–1408, doi:10.1016/J.CRTE.2005.10.006.

George, R., Rogers, N., and Kelley, S., 1998, Earliest magmatism in Ethiopia: Evidence for two mantle plumes in one flood basalt province: Geology, v. 26, p. 923–926, doi:10.1130/0091-7613(1998)026<0923:EMIEEF>2.3.CO;2.

Giannerini, G., Campredon, R., Feraud, G., and Abou Zakhem, B., 1988, Deformations intraplaques et volcanisme associe; exemple de la bordure NW de la plaque Arabique au Cenozoique: Bulletin de la Société Géologique de France, v. IV, p. 937–947, doi:10.2113/gssgfbull.IV.6.937.

Gillard, M., Leroy, S., Cannat, M., and Sloan, H., 2021, Margin-to-Margin Seafloor Spreading in the Eastern Gulf of Aden: A 16 Ma-Long History of Deformation and Magmatism from Seismic Reflection, Gravity and Magnetic Data: Frontiers in Earth Science, v. 9, p. 628, doi:10.3389/feart.2021.707721.

Gvirtzman, Z., Faccenna, C., and Becker, T.W., 2016, Isostasy, flexure, and dynamic topography: Tectonophysics, v. 683, p. 255–271, doi:10.1016/j.tecto.2016.05.041.

Hill, R.I., 1991, Starting plumes and continental break-up: Earth and Planetary Science Letters, v. 104, p. 398–416, doi:10.1016/0012-821X(91)90218-7.

van Hinsbergen, D.J.J. et al., 2021, A record of plume-induced plate rotation triggering subduction initiation: Nature Geoscience, v. 14, p. 626–630, doi:10.1038/s41561-021-00780-7.

van Hinsbergen, D.J.J., Steinberger, B., Doubrovine, P. V., and Gassmöller, R., 2011, Acceleration and deceleration of India-Asia convergence since the Cretaceous: Roles of mantle plumes and continental collision: Journal of Geophysical Research: Solid Earth, v. 116, p. 6101, doi:10.1029/2010JB008051.

Hofstetter, R., and Beyth, M., 2003, The afar depression: Interpretation of the 1960-2000 earthquakes: Geophysical Journal International, v. 155, p. 715–732, doi:10.1046/j.1365-246X.2003.02080.x.

754 Hughes, G.W., Varol, O., and Beydoun, Z.R., 1991, Evidence for Middle Oligocene rifting of the Gulf of Aden
755 and for Late Oligocene rifting of the southern Red Sea: Marine and Petroleum Geology, v. 8, p. 354–
756 358, doi:10.1016/0264-8172(91)90088-I.

757 Huismans, R.S., Podladchikov, Y.Y., and Cloetingh, S., 2001, Transition from passive to active rifting:
758 Relative importance of asthenospheric doming and passive extension of the lithosphere: Journal of
759 Geophysical Research: Solid Earth, v. 106, p. 11271–11291, doi:10.1029/2000JB900424.

760 Ilani, S., Harlavan, Y., Tarawneh, K., Rabba, I., Weinberger, R., Ibrahim, K., Peltz, S., and Steinitz, G., 2001,
761 New K-Ar ages of basalts from the Harrat Ash Shaam volcanic field in Jordan: Implications for the
762 span and duration of the upper-mantle upwelling beneath the western Arabian plate: Geology, v. 29,
763 p. 171–174, doi:10.1130/0091-7613(2001)029<0171:NKAAOB>2.0.CO;2.

764 Ince, E.S., Barthelmes, F., Reißland, S., Elger, K., Förste, C., Flechtner, F., and Schuh, H., 2019, ICGEM – 15
765 years of successful collection and distribution of global gravitational models, associated services, and
766 future plans: Earth System Science Data, v. 11, p. 647–674, doi:10.5194/essd-11-647-2019.

767 Issachar, R., Ebbing, J., and Dilixiati, Y., 2022, New magnetic anomaly map for the Red Sea reveals
768 transtensional structures associated with rotational rifting: Scientific Reports, v. 12, p. 1–13,
769 doi:10.1038/s41598-022-09770-0.

770 Ivanov, A. V., Demonterova, E.I., He, H., Perepelov, A.B., Travin, A. V., and Lebedev, V.A., 2015, Volcanism
771 in the Baikal rift: 40years of active-versus-passive model discussion: Earth-Science Reviews, v. 148,
772 p. 18–43, doi:10.1016/j.earscirev.2015.05.011.

773 Joffe, S., and Garfunkel, Z., 1987, Plate kinematics of the Red Sea – a re-evaluation: Teconophysics, v. 141,
774 p. 5–22.

775 Jolivet, L., and Faccenna, C., 2000, Mediterranean extension and the Africa-Eurasia collision: Tectonics, v.
776 19, p. 1095–1106, doi:10.1029/2000TC900018.

777 Keen, C.E., 1985, The dynamics of rifting: deformation of the lithosphere by active and passive driving
778 forces: Geophys. J. R. ash. Soc, v. 80, p. 95–120,
779 https://academic.oup.com/gji/article/80/1/95/610547 (accessed August 2021).

780 Keir, D., Bastow, I.D., Pagli, C., and Chambers, E.L., 2013, The development of extension and magmatism
781 in the Red Sea rift of Afar: Tectonophysics, v. 607, p. 98–114, doi:10.1016/j.tecto.2012.10.015.

782 Keir, D., Pagli, C., Bastow, I.D., and Ayele, A., 2011, The magma-assisted removal of Arabia in Afar: Evidence
783 from dike injection in the Ethiopian rift captured using InSAR and seismicity: Tectonics, v. 30,
784 doi:https://doi.org/10.1029/2010TC002785.

785 Keranen, K., and Klemperer, S.L., 2008, Discontinuous and diachronous evolution of the Main Ethiopian
786 Rift : Implications for development of continental rifts: Earth and Planetary Science Letters, v. 265, p.
787 96–111, doi:10.1016/j.epsl.2007.09.038.

788 Kidane, T., 2016, Strong clockwise block rotation of the Ali-Sabieh/Aïsha Block: Evidence for opening of the
789 Afar Depression by a “saloon-door” mechanism, *in* Geological Society Special Publication, Geological
790 Society of London, v. 420, p. 209–219, doi:10.1144/SP420.10.

791 Koppers, A.A.P., Becker, T.W., Jackson, M.G., Konrad, K., Müller, R.D., Romanowicz, B., Steinberger, B., and
792 Whittaker, J.M., 2021, Mantle plumes and their role in Earth processes: Nature Reviews Earth &
793 Environment, v. 2, p. 382–401, doi:10.1038/s43017-021-00168-6.

794 Koptev, A., Gerya, T., Calais, E., Leroy, S., and Burov, E., 2018, Afar triple junction triggered by plume-
795 assisted bi-directional continental break-up: Scientific Reports, v. 8, p. 1–7, doi:10.1038/s41598-018-

33117-3.

Leroy, S. et al., 2013, From rifting to oceanic spreading in the Gulf of Aden: A synthesis: Frontiers in Earth Sciences, v. 5, p. 385–427, doi:10.1007/978-3-642-30609-9_20.

Lithgow-Bertelloni, C., and Silver, P.G., 1998, Dynamic topography, plate driving forces and the African superswell: Nature, v. 395, p. 269–272, doi:10.1038/26212.

Macdonald, K., Sempere, J.C., and Fox, P.J., 1984, East Pacific Rise from Siqueiros to Orozco fracture zones: along- strike continuity of axial neovolcanic zone and structure and evolution of overlapping spreading centers.: Journal of Geophysical Research, v. 89, p. 6049–6069, doi:10.1029/JB089iB07p06049.

Maestrelli, D., Brune, S., Corti, G., Keir, D., Muluneh, A.A., and Sani, F., 2022, Analog and Numerical Modeling of Rift-Rift-Rift Triple Junctions: Tectonics, v. 41, p. e2022TC007491, doi:https://doi.org/10.1029/2022TC007491.

Manighetti, I., Tapponnier, P., Courtillot, V., Gallet, Y., Jacques, E., and Gillot, P.Y., 2001, Strain transfer between disconnected, propagating rifts in Afar: Journal of Geophysical Research: Solid Earth, v. 106, p. 13613–13665, doi:10.1029/2000jb900454.

Mattash, M.A., Pinarelli, L., Vaselli, O., Minissale, A., Al-Kadasi, M., Shawki, M.N., and Tassi, F., 2013, Continental Flood Basalts and Rifting: Geochemistry of Cenozoic Yemen Volcanic Province: International Journal of Geosciences, v. 04, p. 1459–1466, doi:10.4236/ijg.2013.410143.

McConnell, R., and Baker, B., 1970, The Structural Pattern of the Afro-Arabian Rift System in Relation to Plate Tectonics: Discussion: Philosophical Transactions of the Royal Society of London Series A, v. 267, p. 390–391, https://www.jstor.org/stable/73628?seq=3#metadata_info_tab_contents (accessed August 2021).

McDougall, I. an, and Brown, F.H., 2009, Timing of volcanism and evolution of the northern Kenya Rift: Geological Magazine, v. 146, p. 34–47, doi:DOI: 10.1017/S0016756808005347.

Meshesha, D., and Shinjo, R., 2008, Rethinking geochemical feature of the Afar and Kenya mantle plumes and geodynamics implications: Journal of Geophysical Research: Solid Earth, v. 113, p. 9209, doi:10.1029/2007JB005549.

Mitchell, N.C., and Bosworth, (in press), W. The tectonic stability of Arabia, *in* Rasul, N.M.A. and Stewart, I.C.F. eds., The tectonic stability of Arabia, in Rifting and sediments in the Red Sea and Arabian Gulf regions, Taylor & Francis.

Mitchell, N.C., and Sofianos, S.S., 2018, Origin of submarine channel north of hanish sill, red sea, *in* Geological Setting, Palaeoenvironment and Archaeology of the Red Sea, Springer International Publishing, p. 259–273, doi:10.1007/978-3-319-99408-6_12.

Mitra, S., Mitra, K., Gupta, S., Bhattacharya, S., Chauhan, P., and Jain, N., 2017, Alteration and submergence of basalts in Kachchh, Gujarat, India: implications for the role of the Deccan Traps in the India–Seychelles break-up: Geological Society, London, Special Publications, v. 445, p. 47–67, doi:10.1144/SP445.9.

Morag, N., Haviv, I., Eyal, M., Kohn, B.P., and Feinstein, S., 2019, Early flank uplift along the Suez Rift: Implications for the role of mantle plumes and the onset of the Dead Sea Transform: Earth and Planetary Science Letters, v. 516, p. 56–65, doi:10.1016/j.epsl.2019.03.002.

Moretti, I., and Froidevaux, C., 1986, Thermomechanical models of active rifting: Tectonics, v. 5, p. 501–511, doi:10.1029/TC005I004P00501.

838 Morgan, W.J., 1971, Convection plumes in the lower mantle: Nature, v. 230, p. 42–43,
839 doi:10.1038/230042a0.

840 Okwokwo, O.I., Mitchell, N.C., Shi, W., Stewart, I.C.F., and Izzeldin, A.Y., 2022, How have thick evaporites
841 affected early seafloor spreading magnetic anomalies in the Central Red Sea? Geophysical Journal
842 International, v. 229, p. 1550–1566, doi:10.1093/gji/ggac012.

843 Pagli, C., Wang, H., Wright, T.J., Calais, E., and Lewi, E., 2014, Current plate boundary deformation of the
844 Afar rift from a 3-D velocity field inversion of InSAR and GPS: Journal of Geophysical Research: Solid
845 Earth, v. 119, p. 8562–8575, doi:https://doi.org/10.1002/2014JB011391.

846 Pagli, C., Yun, S.-H., Ebinger, C., Keir, D., and Wang, H., 2018, Strike-slip tectonics during rift linkage:
847 Geology, v. 47, p. 31–34, doi:10.1130/G45345.1.

848 Peate, I.U., Baker, J.A., Al-Kadasi, M., Al-Subbary, A., Knight, K.B., Riisager, P., Thirlwall, M.F., Peate, D.W.,
849 Renne, P.R., and Menzies, M.A., 2005, Volcanic stratigraphy of large-volume silicic pyroclastic
850 eruptions during Oligocene Afro-Arabian flood volcanism in Yemen: Bulletin of Volcanology, v. 68, p.
851 135–156, doi:10.1007/s00445-005-0428-4.

852 Le Pichon, X., and Gaulier, J.-M., 1988, The rotation of Arabia and the Levant fault system: Tectonophysics,
853 v. 153, p. 271–294, doi:10.1016/0040-1951(88)90020-0.

854 Plaziat, J.-C., Baltzer, F., Choukri, A., Conchon, O., Freytet, P., Orszag-Sperber, F., Raguideau, A., and Reyss,
855 J.-L., 1998, Quaternary marine and continental sedimentation in the northern Red Sea and Gulf of
856 Suez (Egyptian coast): influences of rift tectonics, climatic changes and sea-level fluctuations, *in*
857 Sedimentation and Tectonics in Rift Basins Red Sea:- Gulf of Aden, Springer Netherlands, p. 537–573,
858 doi:10.1007/978-94-011-4930-3_29.

859 Prave, A.R., Bates, C.R., Donaldson, C.H., Toland, H., Condon, D.J., Mark, D., and Raub, T.D., 2016, Geology
860 and geochronology of the Tana Basin, Ethiopia: LIP volcanism, Super eruptions and Eocene-Oligocene
861 environmental change: Earth and Planetary Science Letters, v. 443, p. 1–8,
862 doi:10.1016/j.epsl.2016.03.009.

863 Pusok, A.E., and Stegman, D.R., 2020, The convergence history of India-Eurasia records multiple
864 subduction dynamics processes: Science Advances, v. 6,
865 doi:10.1126/SCIADV.AAZ8681/SUPPL_FILE/AAZ8681_SM.PDF.

866 Qaysi, S., Liu, K.H., and Gao, S.S., 2018, A Database of Shear-Wave Splitting Measurements for the Arabian
867 Plate: Seismological Research Letters, v. 89, p. 2294–2298, doi:10.1785/0220180144.

868 Reilinger, R. et al., 2006, GPS constraints on continental deformation in the Africa-Arabia-Eurasia
869 continental collision zone and implications for the dynamics of plate interactions: Journal of
870 Geophysical Research-Solid Earth, v. 111.

871 Reilinger, R., and McClusky, S., 2011, Nubia-Arabia-Eurasia plate motions and the dynamics of
872 Mediterranean and Middle East tectonics: Geophysical Journal International, v. 186, p. 971–979,
873 doi:10.1111/j.1365-246X.2011.05133.x.

874 Richards, M.A., Duncan, R.A., and Courtillot, V.E., 1989, Flood basalts and hot-spot tracks: Plume heads
875 and tails: Science, v. 246, p. 103–107, doi:10.1126/science.246.4926.103.

876 Rime, V., Foubert, A., Ruch, J., and Kidane, T., 2023, Tectonostratigraphic evolution and significance of the
877 Afar Depression: Earth-Science Reviews, v. 244, p. 104519,
878 doi:https://doi.org/10.1016/j.earscirev.2023.104519.

879 Roger, J., Platel, J.P., Cavelier, C., and Bourdillon-de-Grissac, C., 1989, Données nouvelles sur la

stratigraphie et l'histoire géologique du Dhofar (Sultanat d'Oman): Bulletin de la Société géologique de France, v. 2, p. 256–277, In France, abstract in English.

Rooney, T.O., 2017, The Cenozoic magmatism of East-Africa: Part I — Flood basalts and pulsed magmatism: Lithos, v. 286–287, p. 264–301, doi:10.1016/j.lithos.2017.05.014.

Sandwell, D.T., Müller, R.D., Smith, W.H.F., Garcia, E., and Francis, R., 2014, New global marine gravity model from CryoSat-2 and Jason-1 reveals buried tectonic structure: Science, v. 346, p. 65–67, doi:10.1126/SCIENCE.1258213.

Schettino, A., Macchiavelli, C., Pierantoni, P.P., Zanoni, D., and Rasul, N., 2016, Recent kinematics of the tectonic plates surrounding the red sea and gulf of aden: Geophysical Journal International, v. 207, p. 457–480, doi:10.1093/gji/ggw280.

Schettino, A., Macchiavelli, C., and Rasul, N.M.A., 2018, Plate motions around the red sea since the early oligocene, *in* Geological Setting, Palaeoenvironment and Archaeology of the Red Sea, Springer International Publishing, p. 203–220, doi:10.1007/978-3-319-99408-6_9.

Schult, A., 1974, Palaeomagnetism of tertiary volcanic rocks from the Ethiopian southern plateau and the Danakil block: Journal of Geophysics, v. 40, p. 203–212, https://journal.geophysicsjournal.com/JofG/article/view/277 (accessed June 2021).

Sembroni, A., Faccenna, C., Becker, T.W., Molin, P., and Abebe, B., 2016, Long-term, deep-mantle support of the Ethiopia-Yemen Plateau: Tectonics, v. 35, p. 469–488, doi:10.1002/2015TC004000.Received.

Sengör, A.M.C., and Burke, K., 1978, Relative timing of rifting and volcanism on Earth and its tectonic implications: Geophysical Research Letters, v. 5, p. 419–421, doi:10.1029/GL005I006P00419.

Sobolev, S. V., Sobolev, A. V., Kuzmin, D. V., Krivolutskaya, N.A., Petrunin, A.G., Arndt, N.T., Radko, V.A., and Vasiliev, Y.R., 2011, Linking mantle plumes, large igneous provinces and environmental catastrophes: Nature, v. 477, p. 312–316, doi:10.1038/nature10385.

Stamps, D.S., Flesch, L.M., Calais, E., and Ghosh, A., 2014, Current kinematics and dynamics of Africa and the East African Rift System: Journal of Geophysical Research: Solid Earth, v. 119, p. 5161–5186, doi:10.1002/2013JB010717.

Stockli, D.F., and Bosworth, W.B., 2018, Timing of extensional faulting along the magma-poor central and northern red sea rift margin-transition from regional extension to necking along a hyperextended rifted margin, *in* Geological Setting, Palaeoenvironment and Archaeology of the Red Sea, Springer International Publishing, p. 81–111, doi:10.1007/978-3-319-99408-6_5.

Su, H., and Zhou, J., 2020, Timing of Arabia-Eurasia collision: Constraints from restoration of crustal-scale cross-sections: Journal of Structural Geology, v. 135, p. 104041, doi:10.1016/j.jsg.2020.104041.

Szymanski, E., Stockli, D.F., Johnson, P.R., and Hager, C., 2016, Thermochronometric evidence for diffuse extension and two-phase rifting within the Central Arabian Margin of the Red Sea Rift: Tectonics, v. 35, p. 2863–2895, doi:10.1002/2016TC004336.

Tazieff, H.T., Varet, J., Barberi, F., and Giglia, G., 1972, Tectonic significance of the Afar (or Danakil) depression: Nature, v. 235, p. 144–147.

Tesfaye, S., Harding, D.J., and Kusky, T.M., 2003, Early continental breakup boundary and migration of the Afar triple junction, Ethiopia: Bulletin of the Geological Society of America, v. 115, p. 1053–1067, doi:10.1130/B25149.1.

Varet, J., 2018, Geology of Afar (East Africa): 1–249 p.

921 Varet, J., 1978, Geology of central and southern Afar (Ethiopia and Djibouti Republic): Paris, Centre
922 national de la recherche scientifique.

923 Viltres, R., Jónsson, S., Alothman, A.O., Liu, S., Leroy, S., Masson, F., Doubre, C., and Reilinger, R., 2022,
924 Present-Day Motion of the Arabian Plate: Tectonics, v. 41, p. e2021TC007013,
925 doi:https://doi.org/10.1029/2021TC007013.

926 Viltres, R., Jónsson, S., Ruch, J., Doubre, C., Reilinger, R., Floyd, M., and Ogubazghi, G., 2020, Kinematics
927 and deformation of the southern Red Sea region from GPS observations: Geophysical Journal
928 International, v. 221, p. 2143–2154, doi:10.1093/gji/ggaa109.

929 Watchorn, F., Nichols, G.J., and Bosence, D.W.J., 1998, Rift-related sedimentation and stratigraphy,
930 southern Yemen (Gulf of Aden), *in* Sedimentation and Tectonics in Rift Basins Red Sea:- Gulf of Aden,
931 Springer Netherlands, p. 165–189, doi:10.1007/978-94-011-4930-3_11.

932 Wescott, W.A., Wigger, S.T., Stone, D.M., and Morley, C.K., 1999, AAPG Studies in Geology# 44, Chapter 3:
933 Geology and Geophysics of the Lotikipi Plain:

934 White, R., and McKenzie, D., 1989, Magmatism at rift zones: the generation of volcanic continental margins
935 and flood basalts: Journal of Geophysical Research, v. 94, p. 7685–7729,
936 doi:10.1029/JB094iB06p07685.

937 White, R.S., and McKenzie, D., 1995, Mantle plumes and flood basalts: Journal of Geophysical Research, v.
938 100, p. 543–560, doi:10.1029/95jb01585.

939 Will, T.M., and Frimmel, H.E., 2018, Where does a continent prefer to break up? Some lessons from the
940 South Atlantic margins: Gondwana Research, v. 53, p. 9–19, doi:10.1016/j.gr.2017.04.014.

941 Wilson, J.T., 1963, A possible origin of the Hawaiian Islands: Canadian Journal of Physics, v. 41, p. 863–870,
942 doi:10.1139/P63-094.

943 Wolfenden, E., Ebinger, C., Yirgu, G., Deino, A., and Ayalew, D., 2004, Evolution of the northern Main
944 Ethiopian rift: Birth of a triple junction: Earth and Planetary Science Letters, v. 224, p. 213–228,
945 doi:10.1016/j.epsl.2004.04.022.

946 Zingerle, P., Pail, R., Gruber, T., and Oikonomidou, X., 2020, The combined global gravity field model
947 XGM2019e: Journal of Geodesy 2020 94:7, v. 94, p. 1–12, doi:10.1007/S00190-020-01398-0.

948 Zwaan, F., Corti, G., Keir, D., and Sani, F., 2020a, A review of tectonic models for the rifted margin of Afar:
949 Implications for continental break-up and passive margin formation: Journal of African Earth
950 Sciences, v. 164, doi:10.1016/j.jafrearsci.2019.103649.

951 Zwaan, F., Corti, G., Sani, F., Keir, D., Muluneh, A.A., Illsley-Kemp, F., and Papini, M., 2020b, Structural
952 Analysis of the Western Afar Margin, East Africa: Evidence for Multiphase Rotational Rifting:
953 Tectonics, v. 39, doi:10.1029/2019TC006043.

954

955

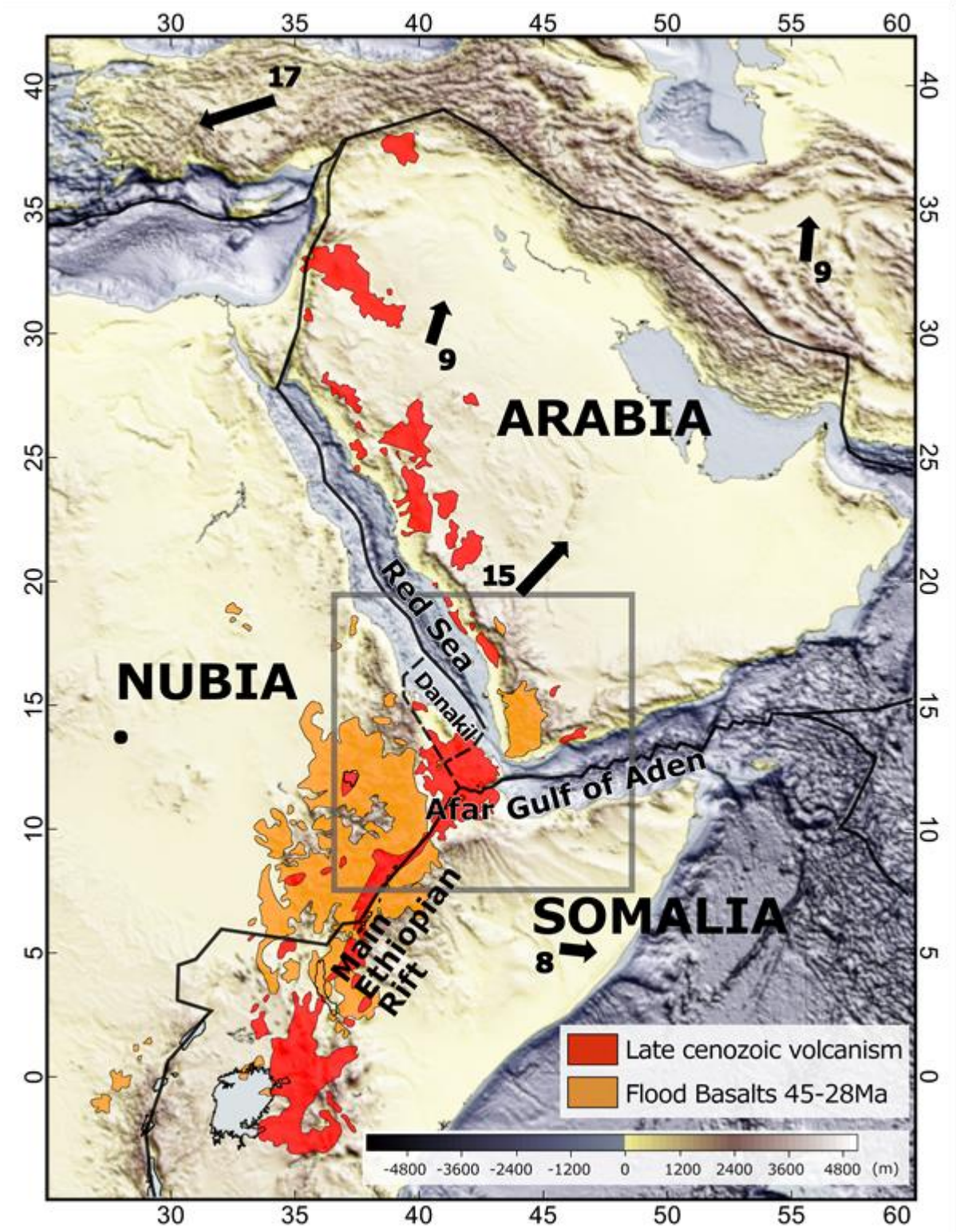

956

957 **Figure 1.** Elevation map of the study area, showing the general plate tectonic configuration (from USGS
958 and from Viltres et al. (2020) in the Afar region) and Cenozoic volcanics (modified from Varet, 1978;
959 Davison et al., 1994; Beyene and Abdelsalam, 2005; Bosworth and Stockli, 2016) Black arrows indicate GPS
960 velocities in respect to Nubia (modified from Reilinger et al., 2006).

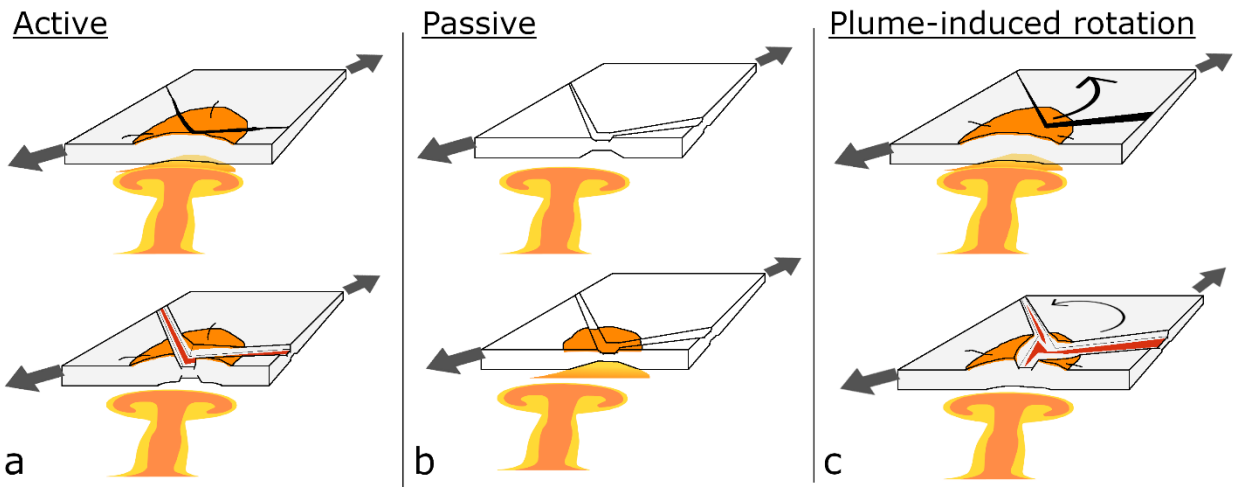

Figure 2. Schematic mechanisms for plume-rift association in the Afro-Arabian rift. (a) Active mechanism, in which rifting results from the actively rising head of the Afar plume. In this mechanism impinging and eroding the base of the lithosphere prompt uplift and decompression melting and flood basalts volcanism. These introduce internal extensional forces and ultimately lead to break-up. (b) Passive mechanism, in which rifting is initiated solely by the remote stresses, regardless of underlying Afar plume. In this mechanism the production of massive volcanism is allowed when the thinned and stretched lithosphere is underlain by the thermal anomaly in the mantle. Flood basalts volcanism is generated by passively rising decompression melting of hot asthenospheric mantle. (c) Plume-induced plate rotation, in which lateral forces, induced by the arrival of the Afar plume head, add up to the remote stresses to change the plate kinematics. In this mechanism flood basalts volcanism is actively controlled, however, rifting is triggered by the new plate kinematics.

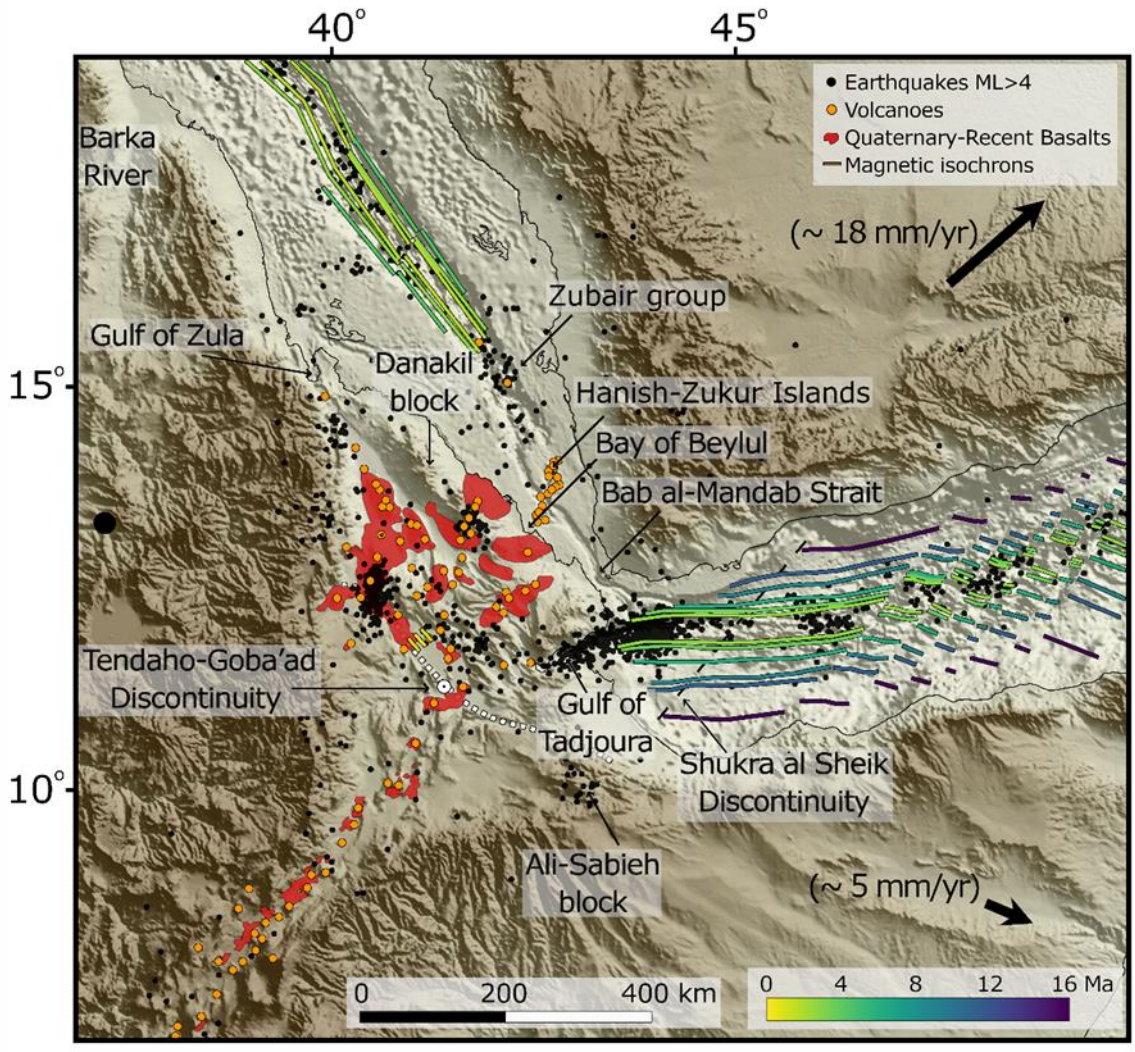

973

974 **Figure 3.** Map of the Afar region showing magnetic isochrons (modified from Fournier et al., 2010; Bridges
975 et al., 2012; Schettino et al., 2016), earthquake locations (from ISC catalog), Holocene onshore volcano
976 locations (from GVP catalog and Viltres et al. (2020)) and recent volcanism (modified from Keir et al., 2013).

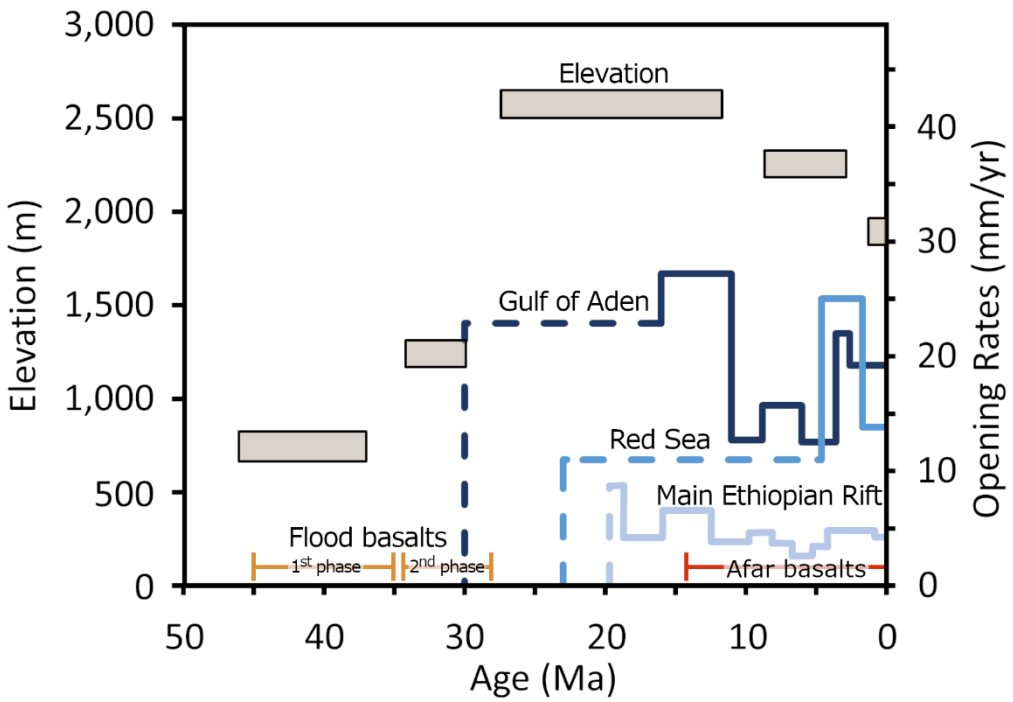

977

978 **Figure 4.** Elevation of the Ethiopian–Yemen plateau (after Sembroni et al., 2016; Faccenna et al., 2019),
979 volcanic episodes and opening rates of the rift arms (modified from Fournier et al., 2010; DeMets and
980 Merkouriev, 2016; Schettino et al., 2018). Dashed lines indicate estimations from geological observations
981 and solid lines from magnetic isochrons.

982

983

984

985

986

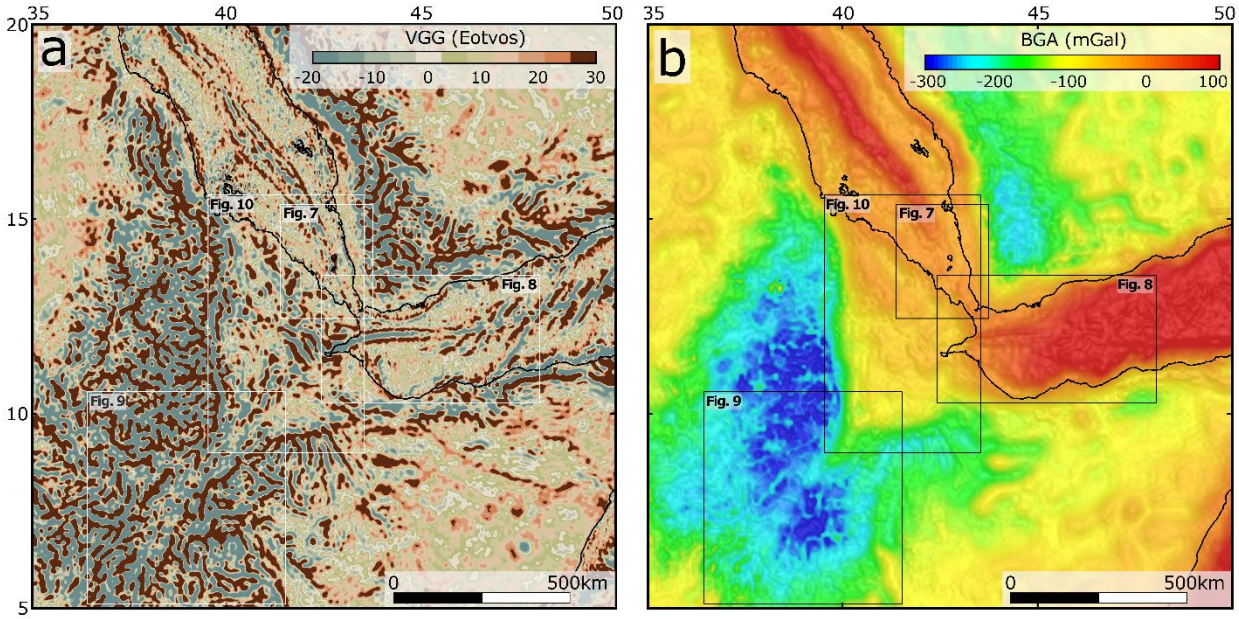

Figure 5. Gravity data of the Afar region. (a) Vertical gravity gradient from Sandwell et al. (2014). (b) Bouguer anomaly model from ICGEM, XGM2019e (Zingerle et al., 2020).

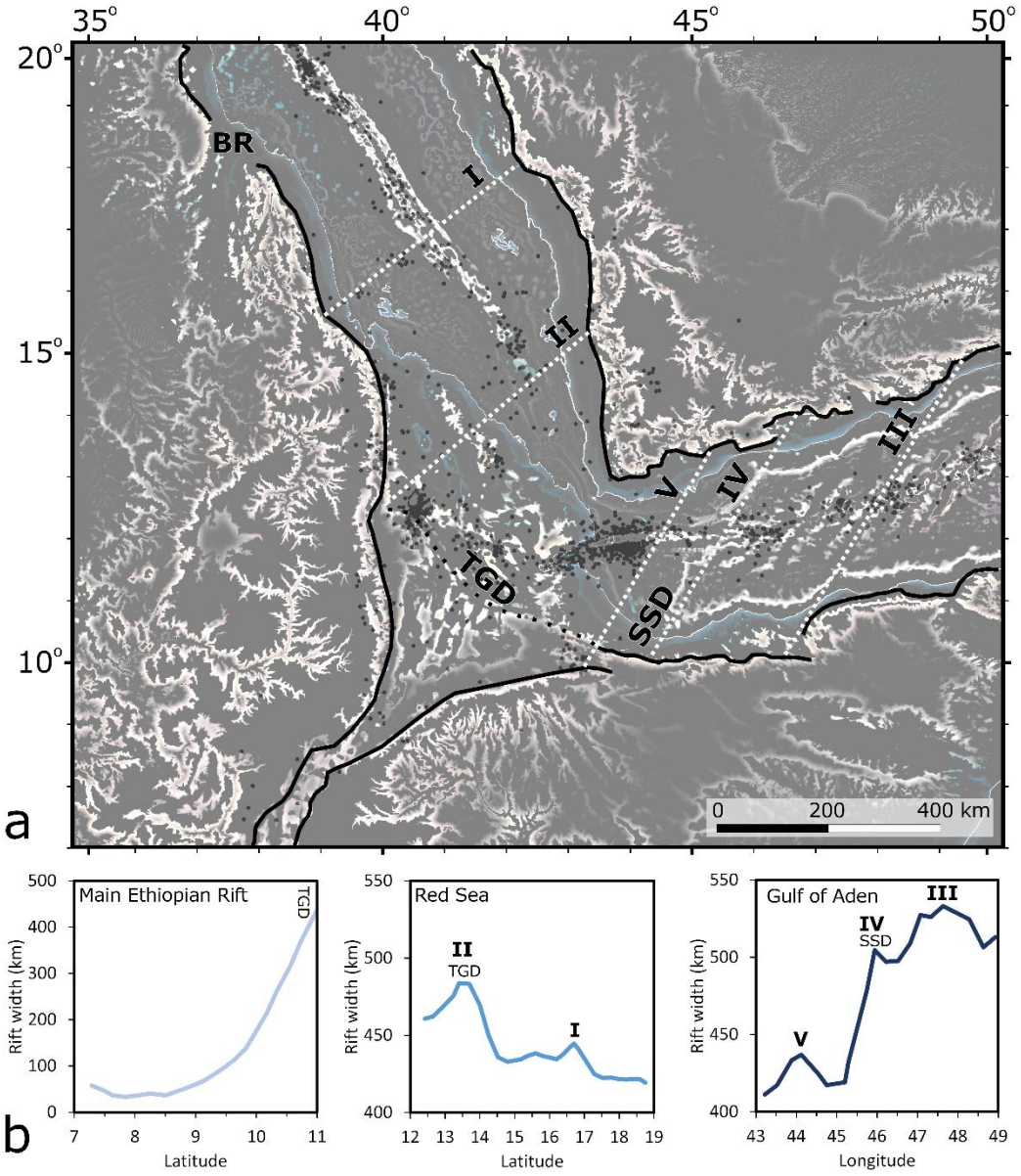

Figure 6. (a) Difference of Gaussians applied to topography and bathymetry showing rift margins (black lines). White dashed lines indicate peaks in rift width. TGD is the Tendaho-Goba'ad Discontinuity. SSD is the Shukra al Sheik discontinuity. Black dots indicate earthquake locations (ISC catalog). (b) Rift widths, calculated in rift-perpendicular directions.

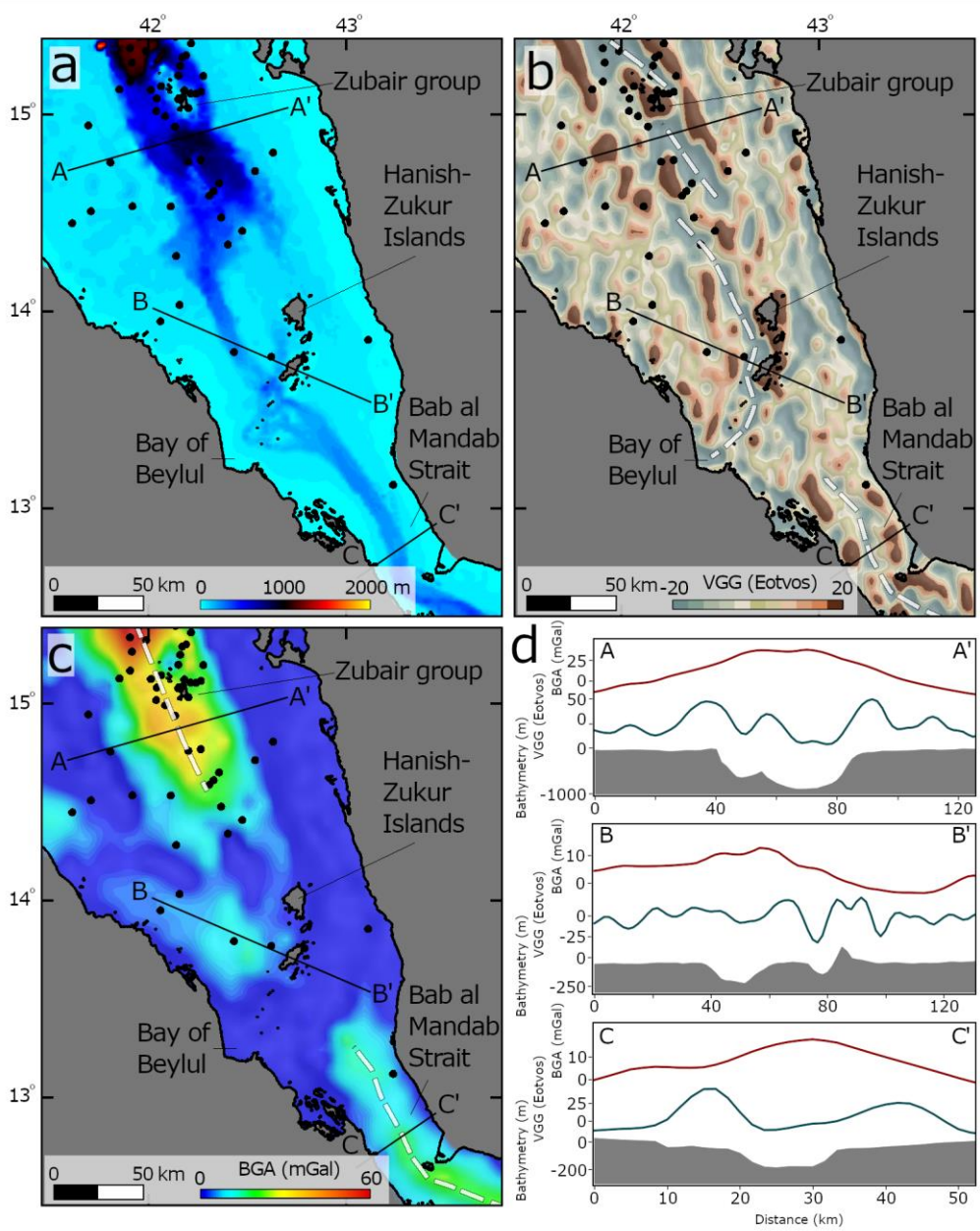

995

996 **Figure 7.** Bathymetry (a), vertical gravity gradient (b) and Bouguer anomaly (c) in the southern Red Sea.
997 Black dots indicate earthquake locations (ISC catalog). (d) Profiles across rift axis.

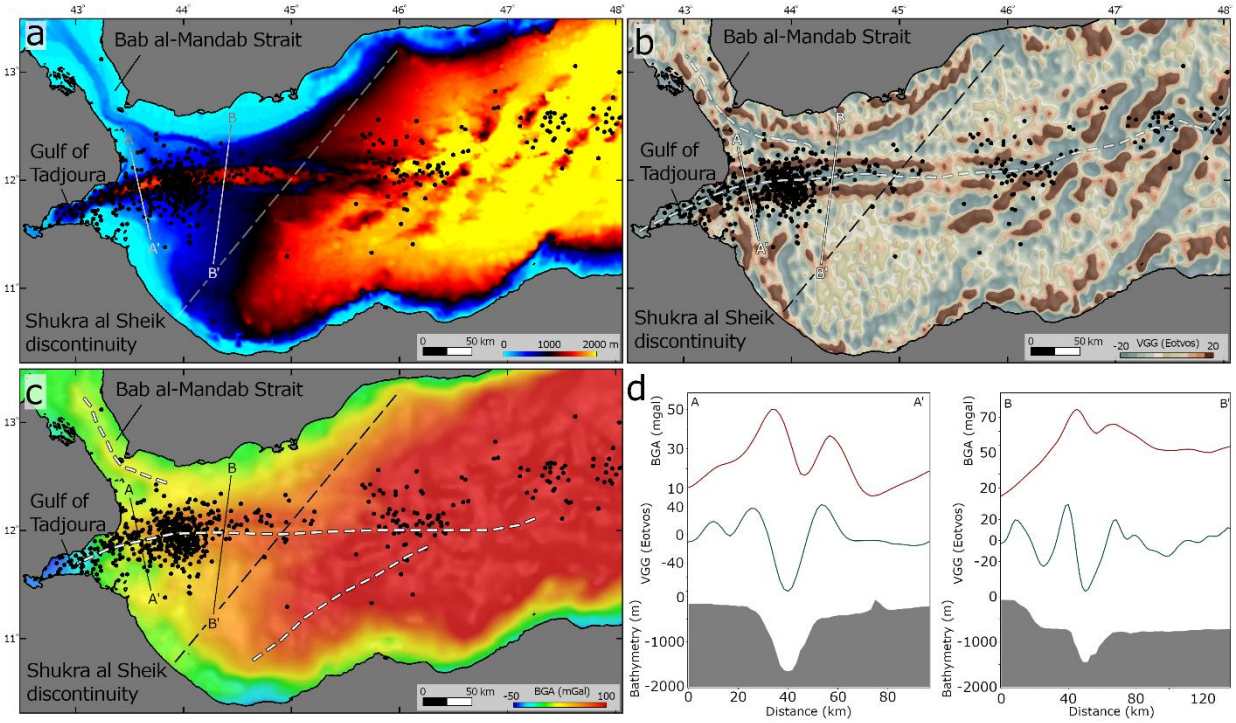

998

999 **Figure 8.** Bathymetry (a), vertical gravity gradient (b) and Bouguer anomaly (c) in the Western Gulf of Aden.
1000 Black dots indicate earthquake locations (ISC catalog). (d) Profiles across rift axis.

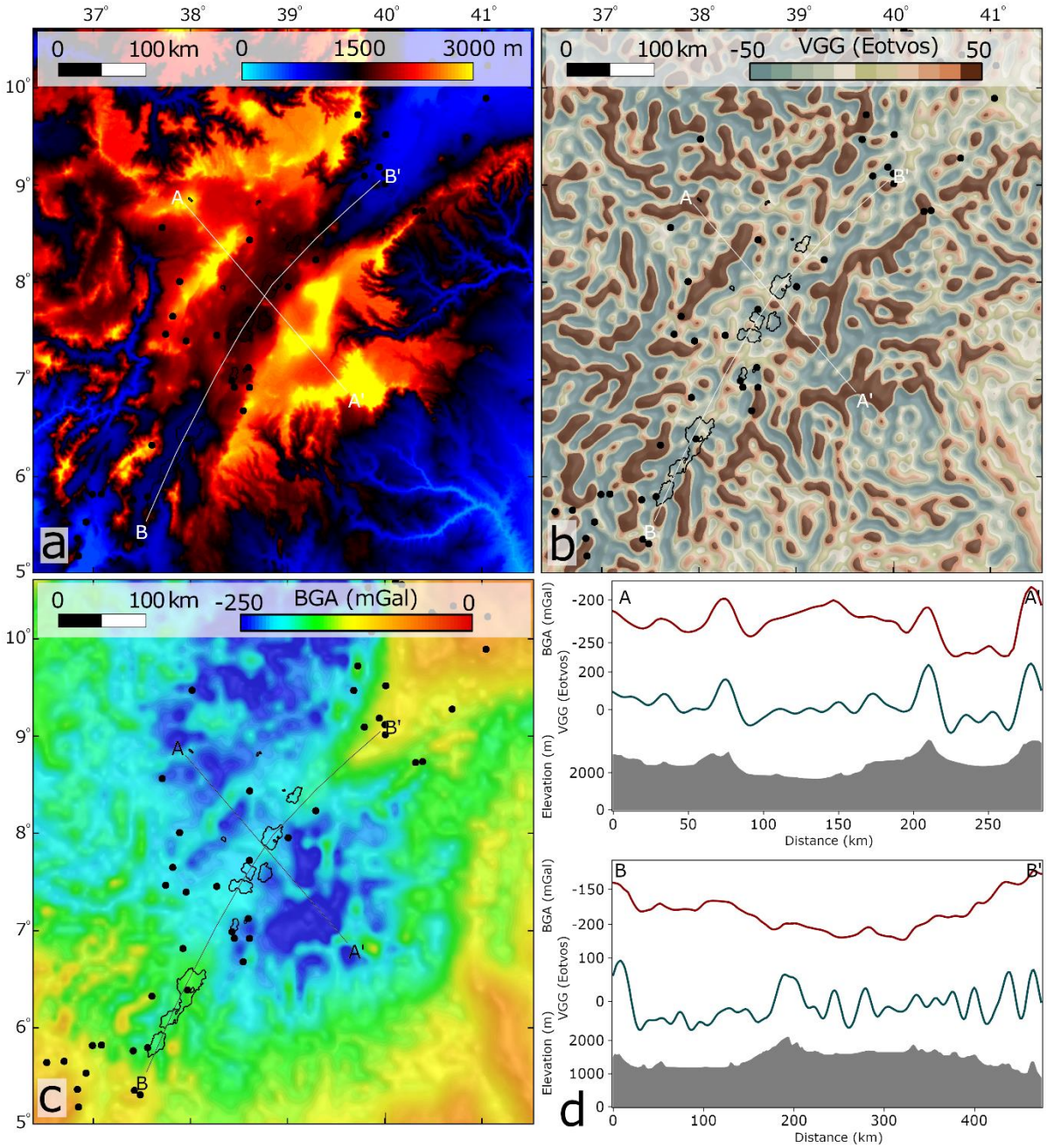

Figure 9. Topography (a), vertical gravity gradient (b) and Bouguer anomaly (c) in the northern Main Ethiopian Rift. Black dots indicate earthquake locations (ISC catalog). (d) Profiles across (AA') and along (BB') the rift valley.

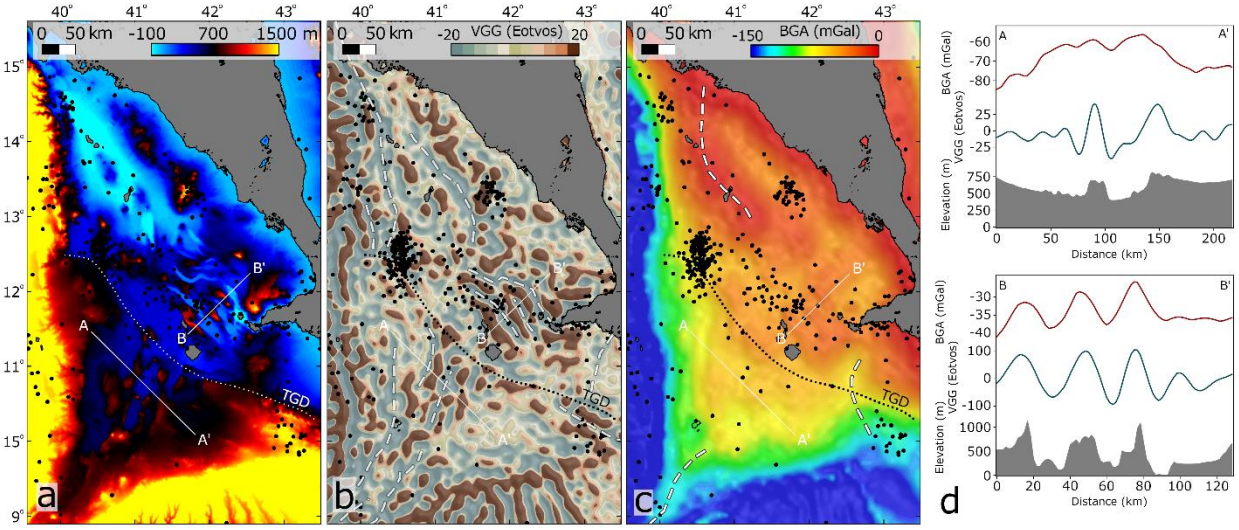

Figure 10. Topography (a), vertical gravity gradient (b) and Bouguer anomaly (c) in the Afar triangle. Black dots indicate earthquake locations (ISC catalog). TGD is the Tendaho-Goba'ad Discontinuity. (d) Profiles SW (AA') and NE (BB') to the TGD.

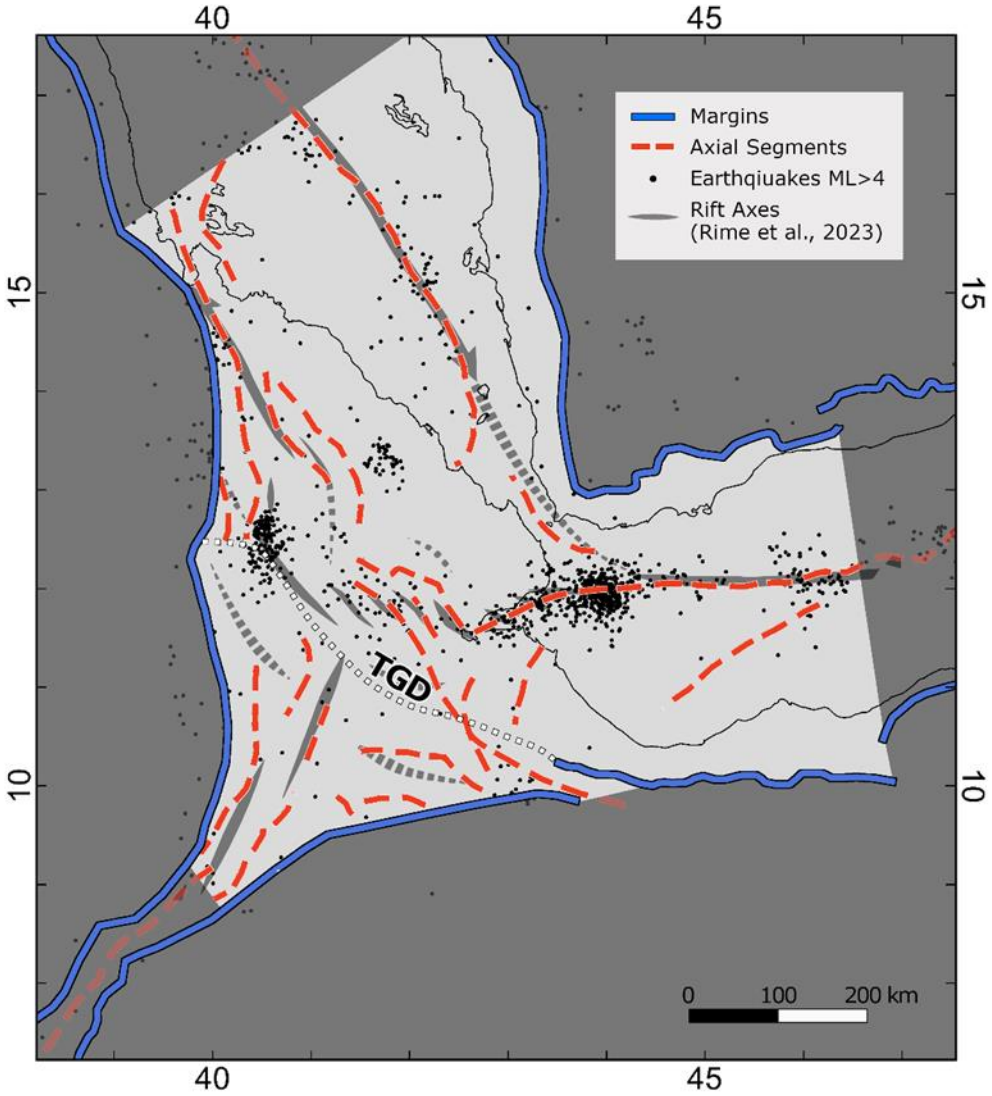

Figure 11. Rift margins and axial segments in the Afar region. Black dots indicate earthquake locations (ISC catalog). TGD is the Tendaho-Goba'ad Discontinuity. Rift axes based on field observations after Rime et al. (2023).

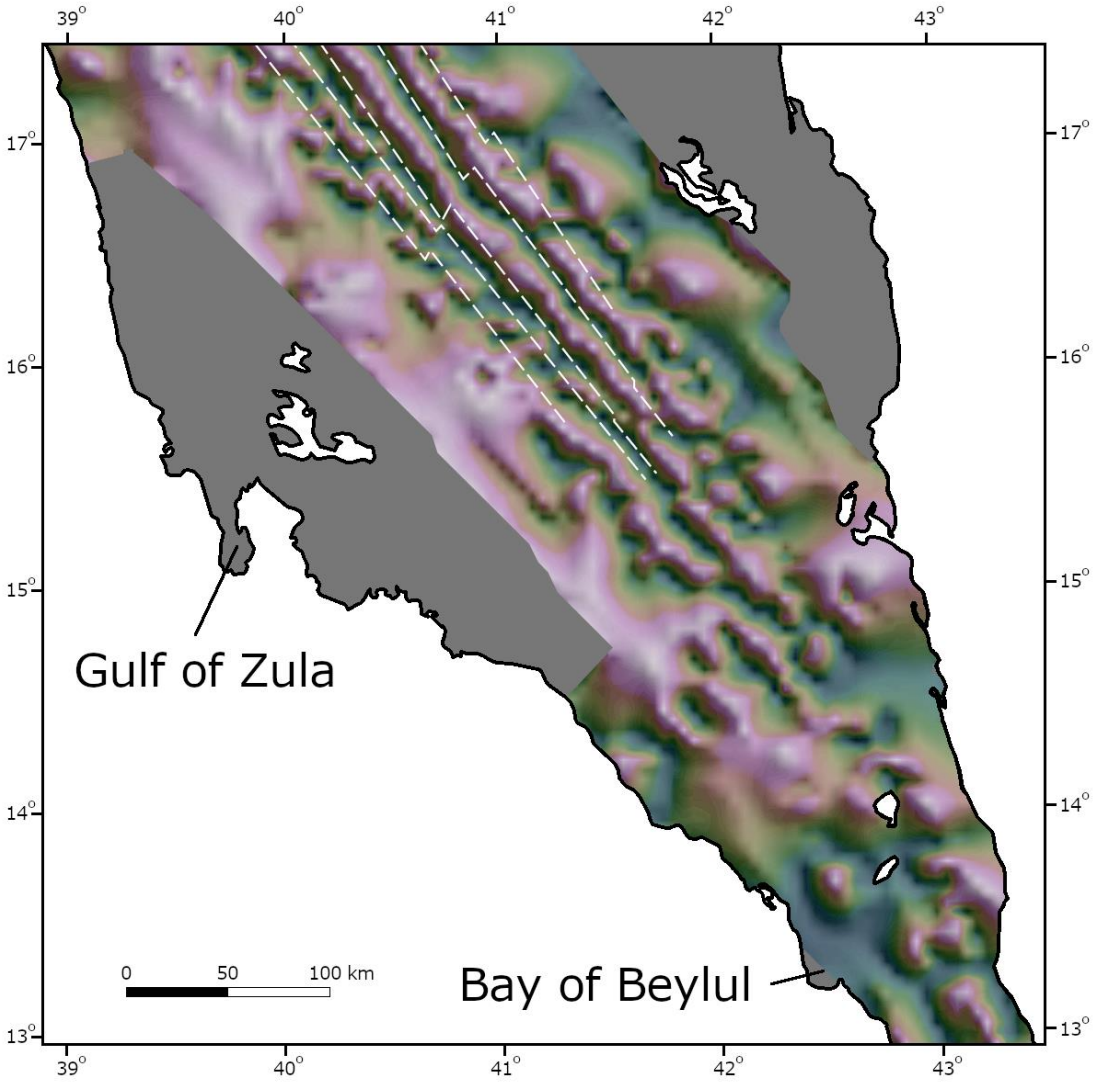

Figure 12. Tilt-angle derivative map of magnetic anomalies, projected on a shaded relief after Issachar et al. (2022). Purple colors represent positive angles and green colors represent negative angles. White dashed lines indicate magnetic stripes (Schettino et al., 2016).

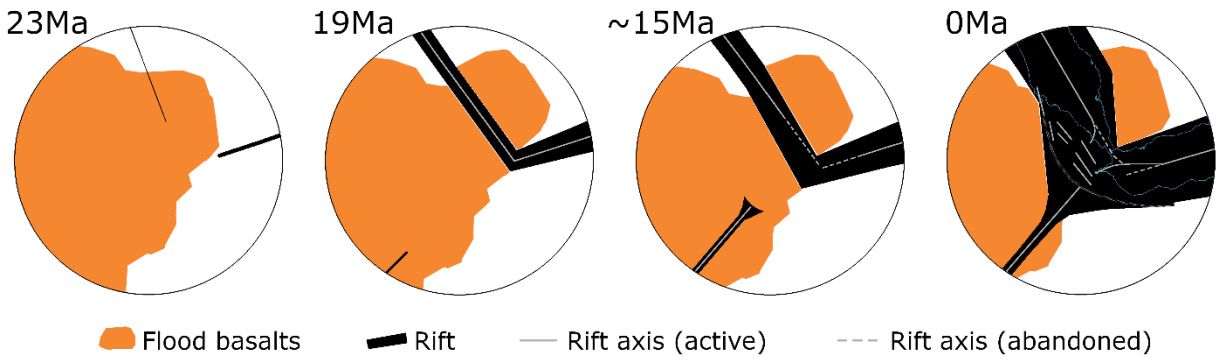

1024

1025 **Figure 13.** Synthesis of the progressive development of the rift intersections.